Positive evidence for Primordial Black Holes

Zooming in on PBH, 4th March 2024

Juan García-Bellido
IFT-UAM/CSIC

Outline

- **Theory:**
  - **Critical Higgs Inflation**
  - **Quantum Diffusion**

- **Observational Evidences:**
  - **Gravitational Lensing**
  - **Gravitational Waves**

Inflation

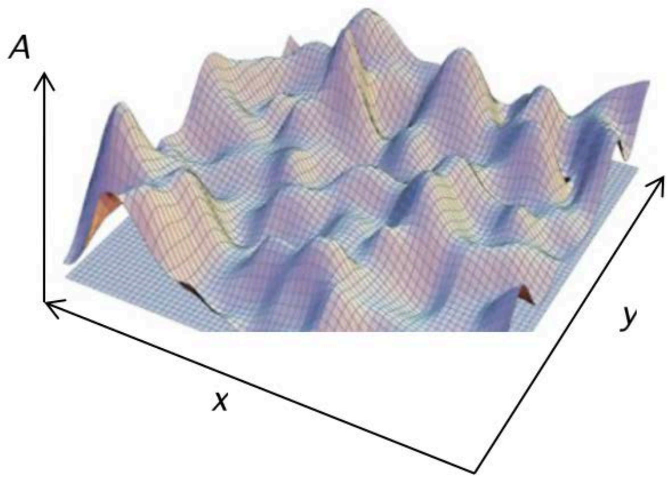

Quantum Fluctuations =
Space-Time Ripples

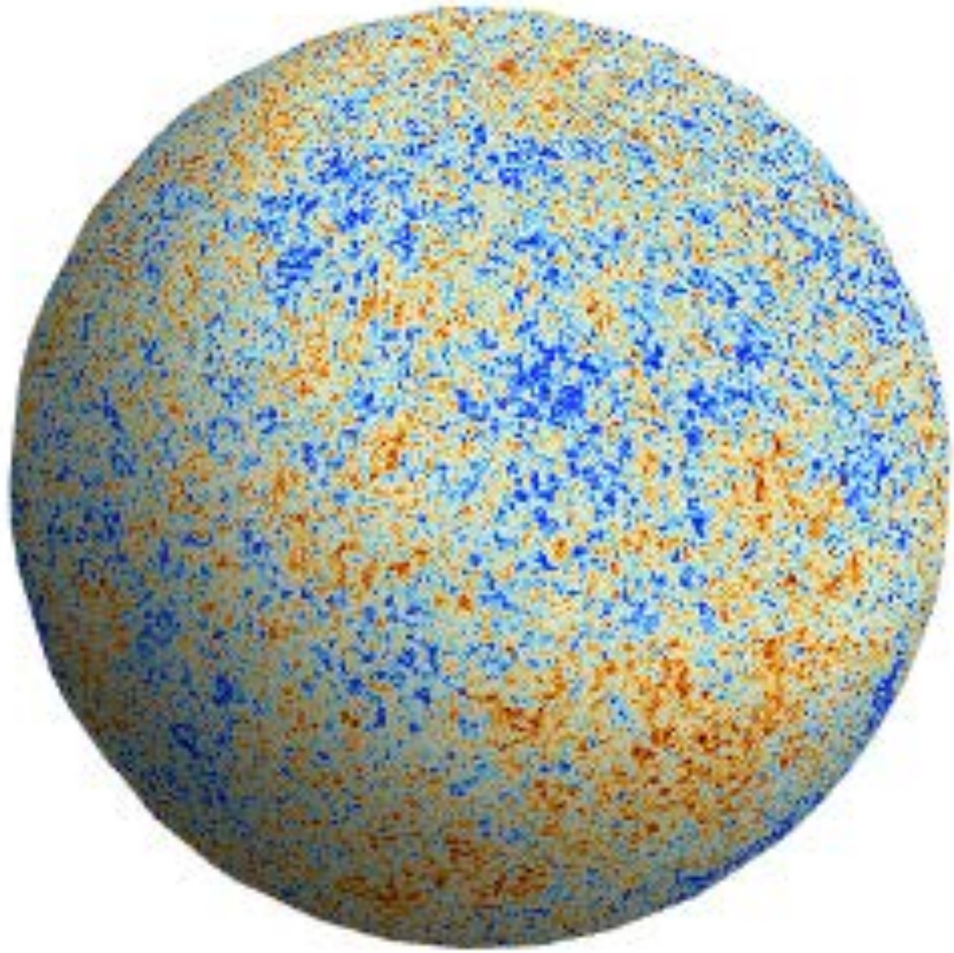

Stretched to cosmological scales

Standard Model Lagrangian

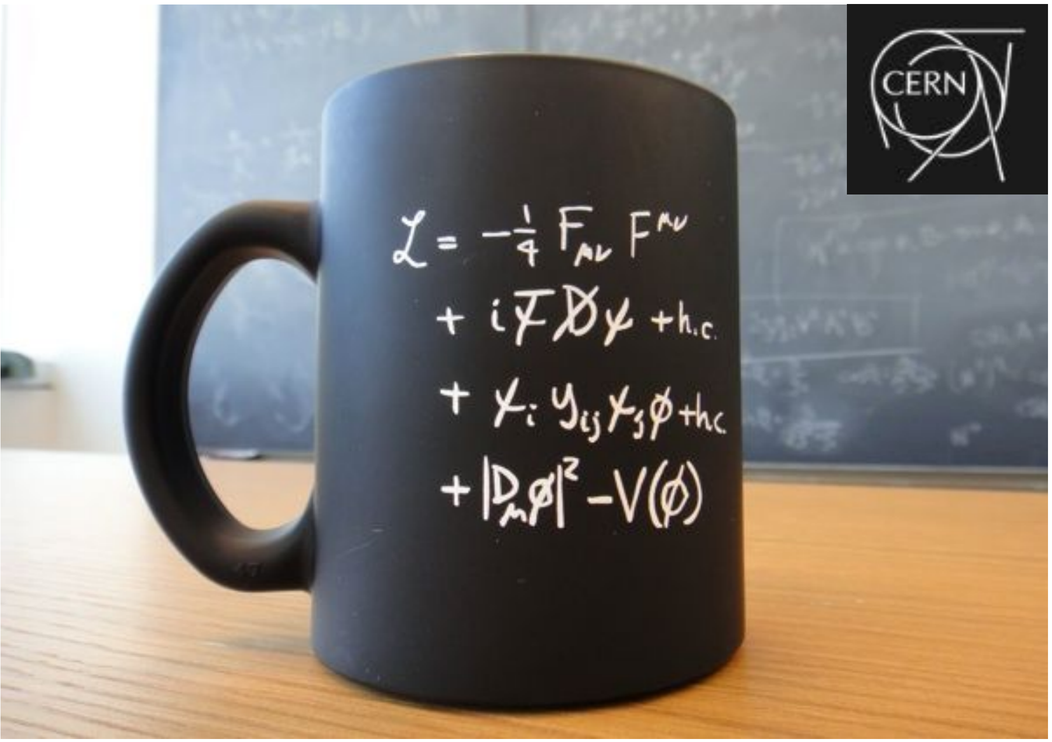

$$
\begin{aligned}
\mathcal{L} = & -\frac{1}{4} F_{\mu\nu} F^{\mu\nu} \\
& + i \bar{\Psi} \not{D} \psi + h.c. \\
& + \bar{\psi}_i y_{ij} \psi_j \phi + h.c. \\
& + |D_\mu \phi|^2 - V(\phi) \\
& + \xi |\phi|^2 R
\end{aligned}
$$

$$R = 12H^2 + 6\dot{H} \rightarrow R_0 = 9.2\, H_0^2 \rightarrow m_H = \sqrt{\xi R_0} = 2 \times 10^{-32}\ \mathrm{eV}$$

EW vacuum metastability

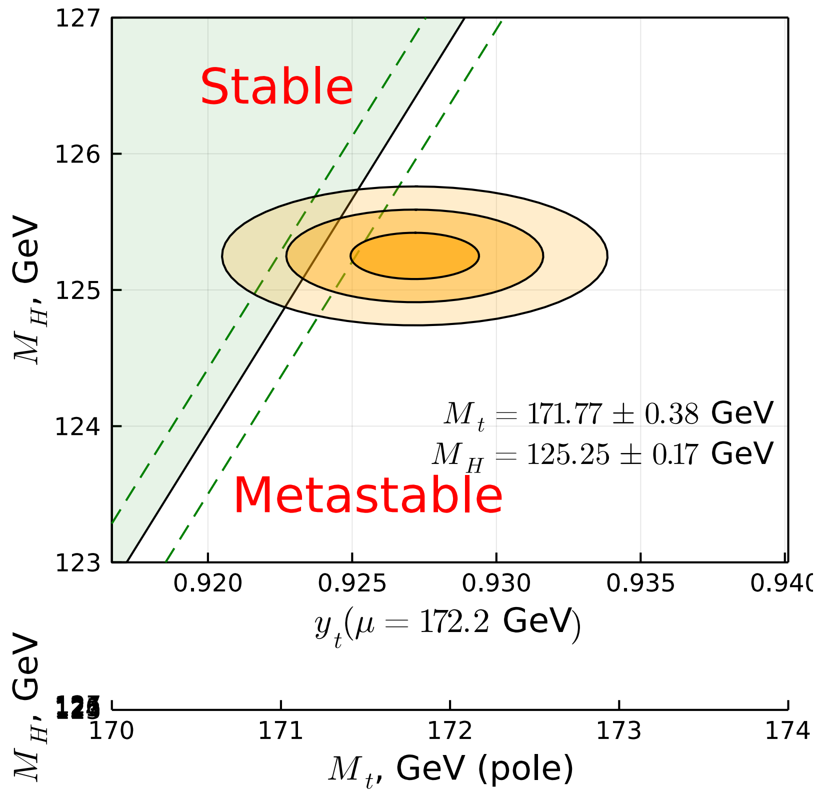

$$m_t^{\text{pole}} = 170.5 \pm 0.8\,\text{GeV}$$

$$\alpha_S(m_Z) = 0.1135^{+0.0021}_{-0.0017}$$

LHC-CMS Collab. (2020)

https://arxiv.org/abs/1904.05237

Buttazzo et al. (2012)

https://arxiv.org/pdf/1112.3022.pdf

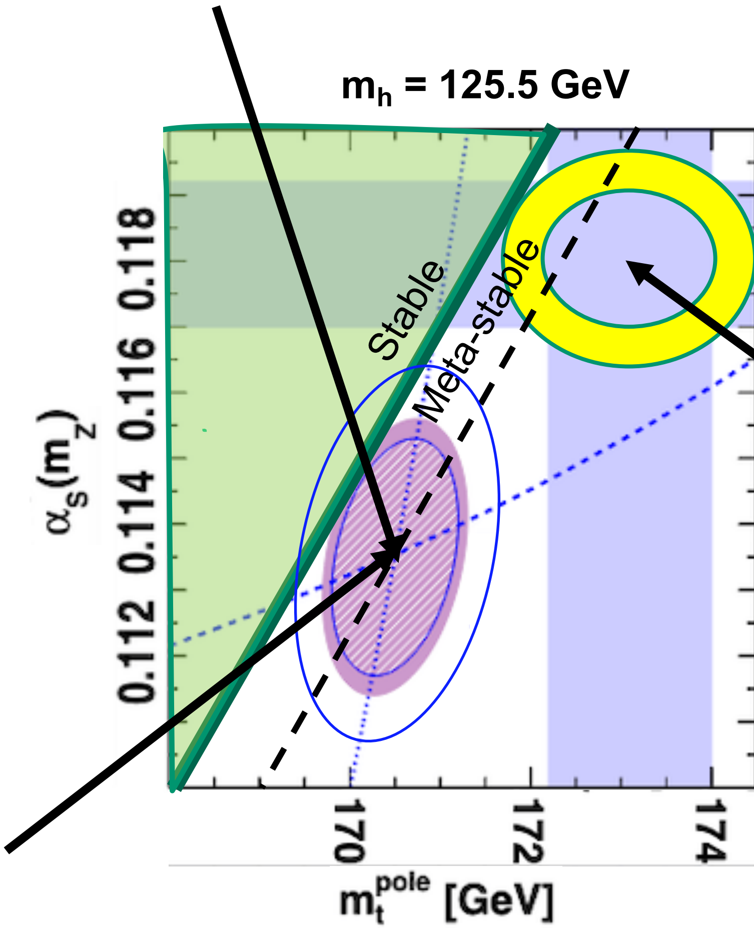

Renormalization of Higgs couplings

Ezquiaga, JGB, Ruiz [1705.04861]

$$\lambda(\phi) = \lambda_0 + b_\lambda \ln^2(\phi/\mu) ,$$
$$\xi(\phi) = \xi_0 + b_\xi \ln(\phi/\mu) ,$$

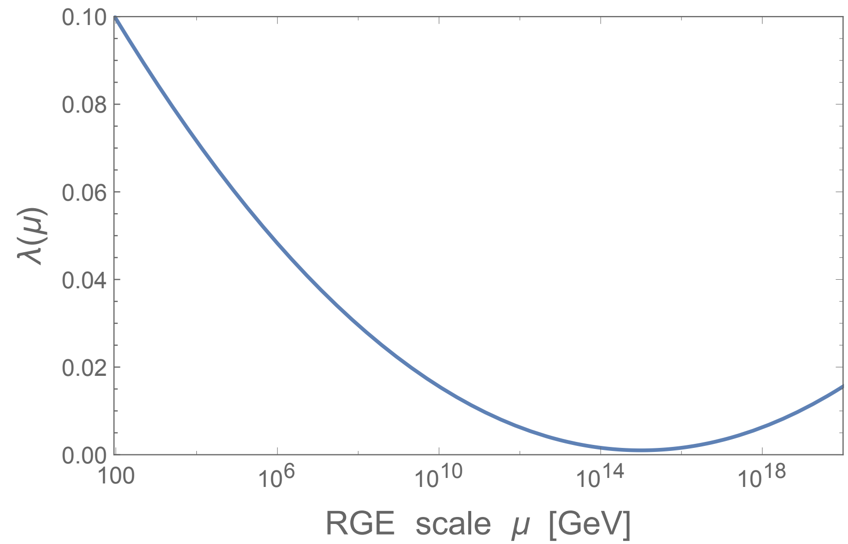

Buttazzo et al (2014)

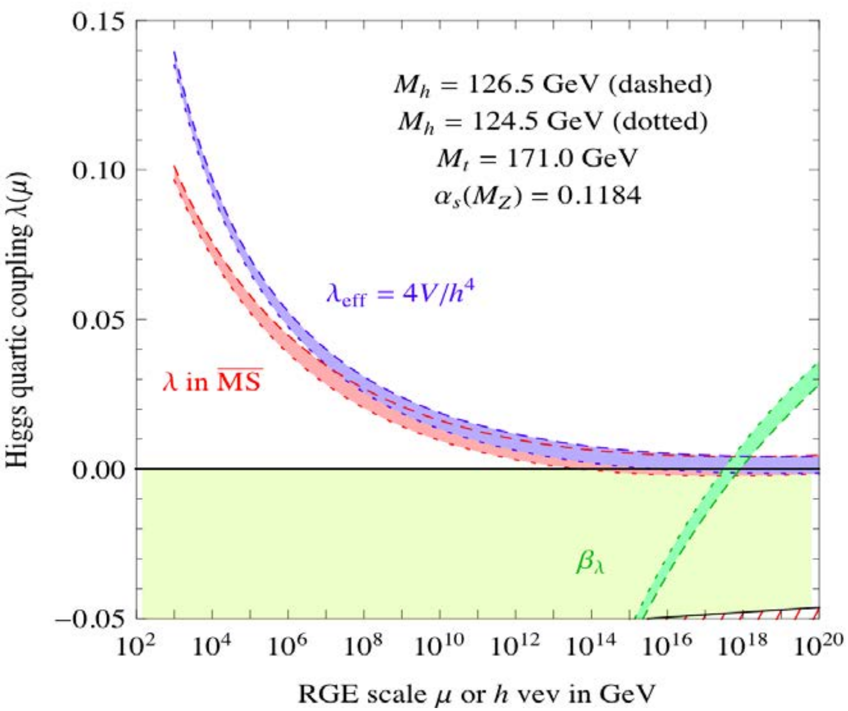

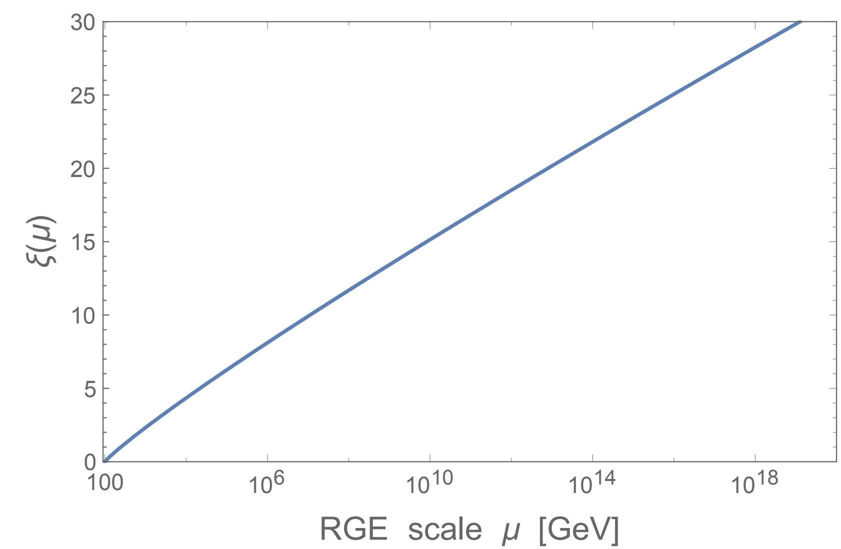

Critical Higgs Inflation

Ezquiaga, JGB, Ruiz Morales [1705.04861]

$$S = \int d^4x \sqrt{g} \left[\left(\frac{1}{2\kappa^2} + \frac{\xi(\phi)}{2}\phi^2 \right) R - \frac{1}{2}(\partial\phi)^2 - \frac{1}{4}\lambda(\phi)\phi^4 \right]$$

$$\lambda(\phi) = \lambda_0 + b_\lambda \ln^2(\phi/\mu) \ ,$$

$$\xi(\phi) = \xi_0 + b_\xi \ln(\phi/\mu) \ ,$$

$$\frac{d\varphi}{d\phi} = \frac{\sqrt{1 + \xi(\phi)\,\phi^2 + 6\,\phi^2\,(\xi(\phi) + \phi\,\xi'(\phi)/2)^2}}{1 + \xi(\phi)\,\phi^2}$$

$$V(x) = \frac{V_0\,(1 + a\,\ln^2 x)\,x^4}{(1 + c\,(1 + b\,\ln x)\,x^2)^2} \qquad x = \phi/\mu$$

$V_0 = \lambda_0\mu^4/4$, $a = b_\lambda/\lambda_0$, $b = b_\xi/\xi_0$ and $c = \xi_0\,\kappa^2\mu^2$

Conformal redefinition of metric and Higgs

$$g_{\mu\nu} \to h_{\mu\nu} = (1 + \xi\phi^2) g_{\mu\nu}$$

$$\phi \to \varphi = \int \frac{\sqrt{1 + \xi(1 + 6\xi)\phi^2}}{1 + \xi\phi^2} d\phi$$

$$V(\phi) \to U(\varphi) = \frac{V(\phi)}{1 + \xi\phi^2}$$

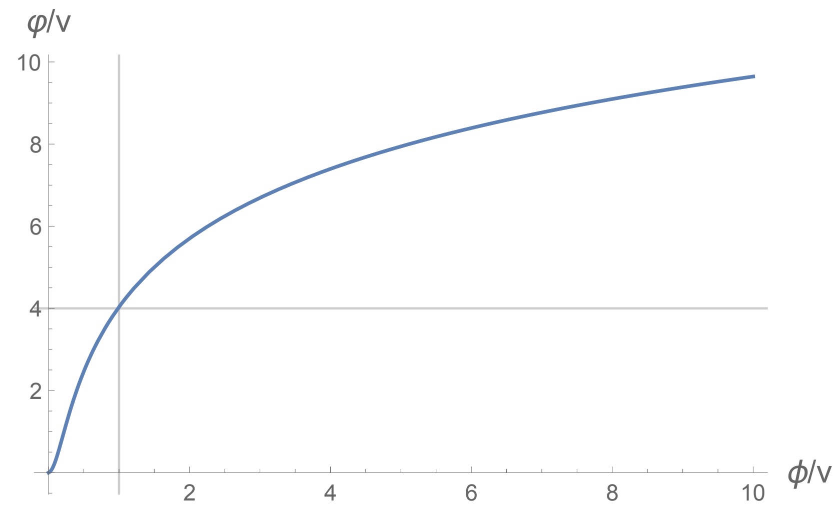

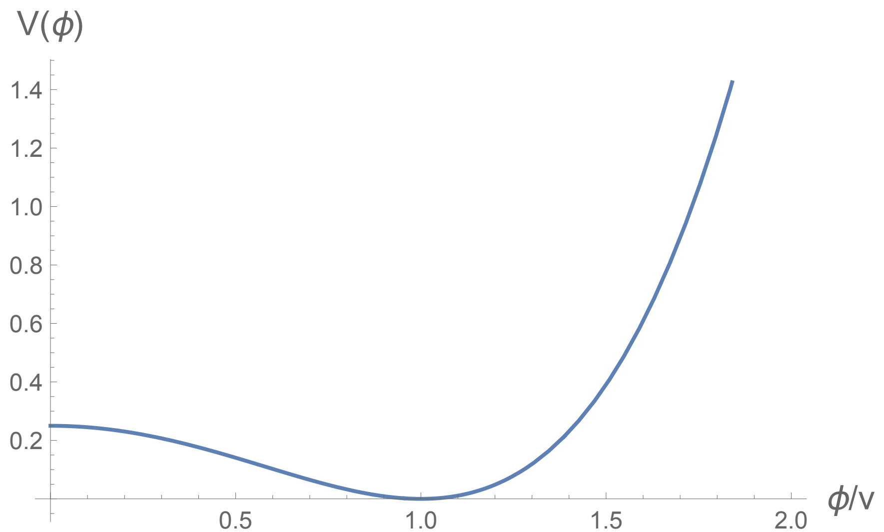

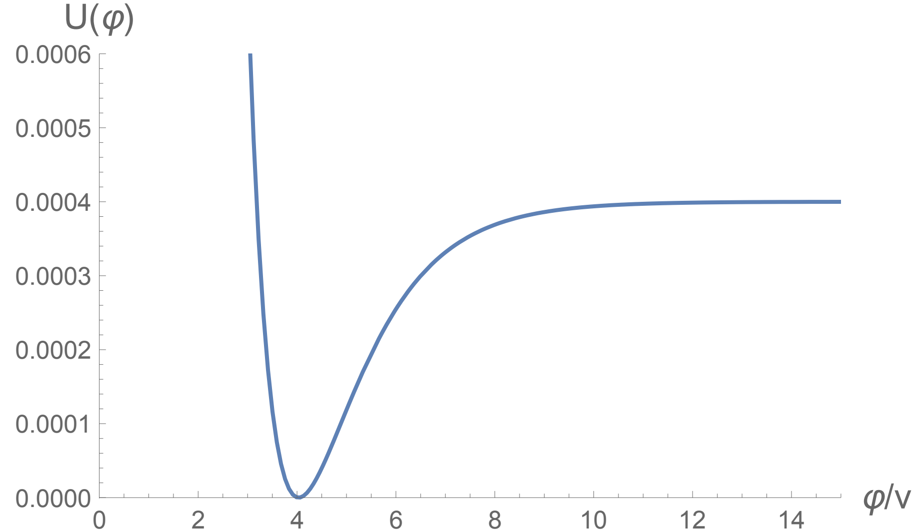

JGB, Ruiz Morales [1702.03901]

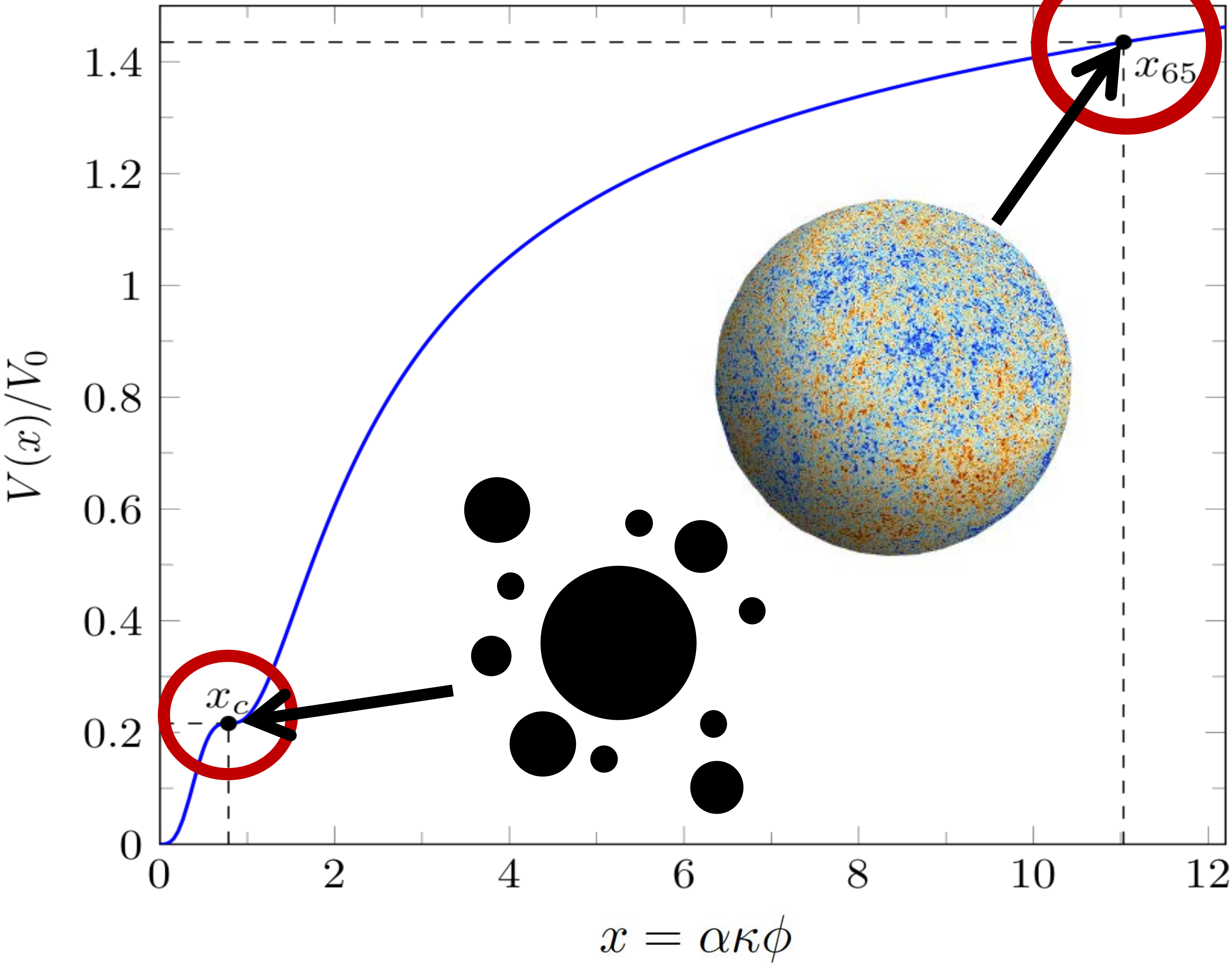

Primordial Power Spectrum

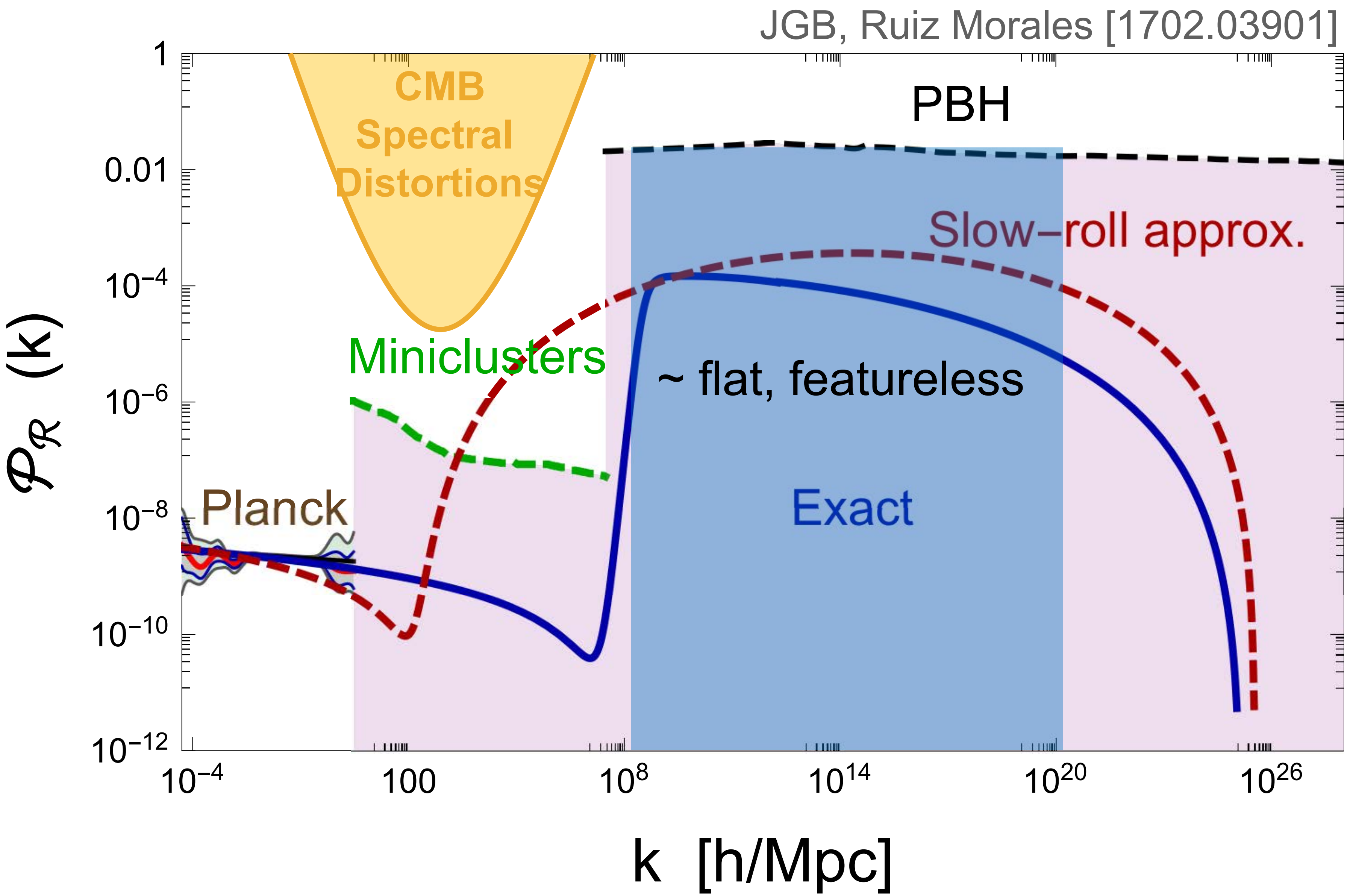

Inflation

JGB [1702.08275]

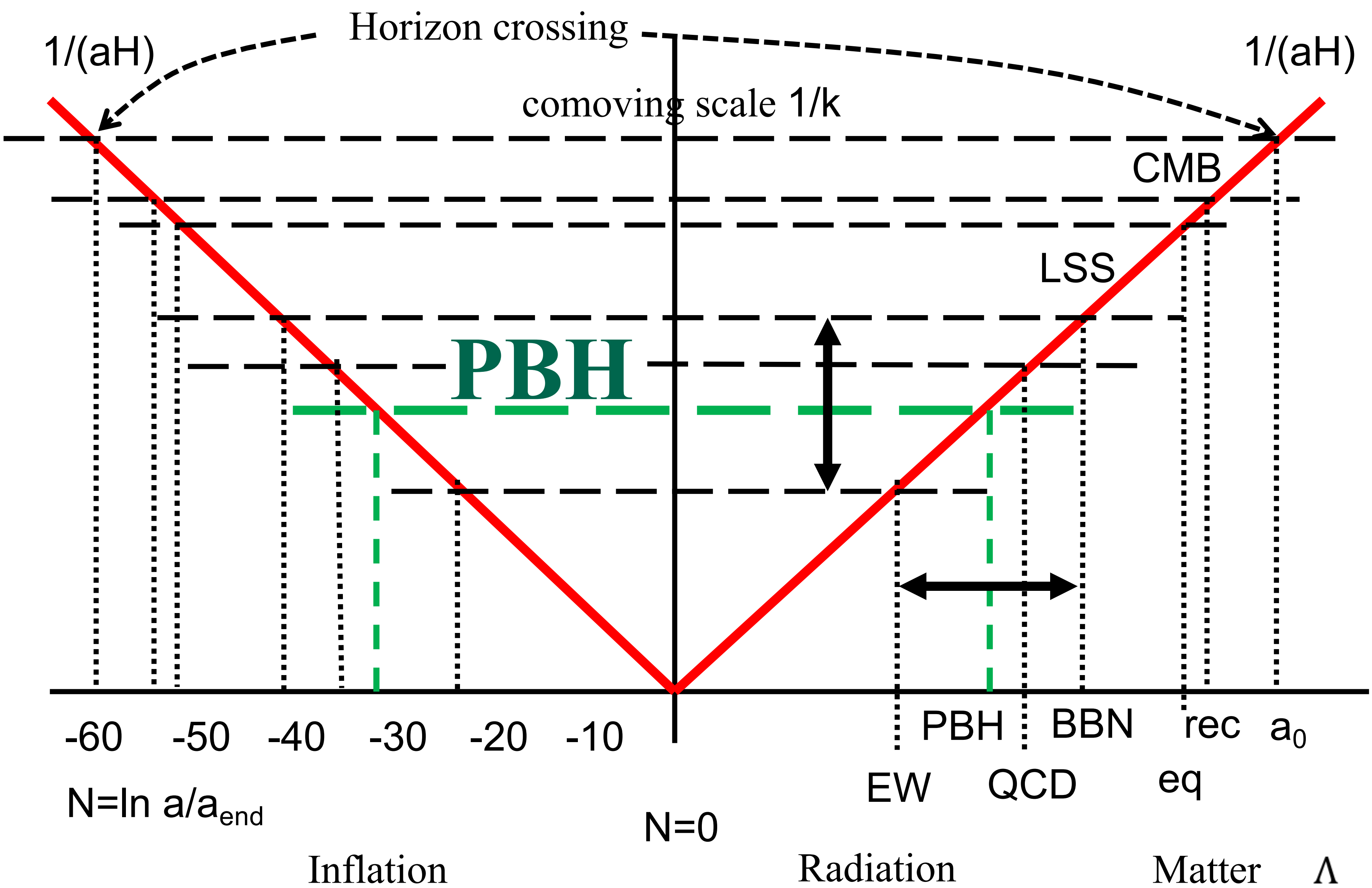

Thermal history of the universe

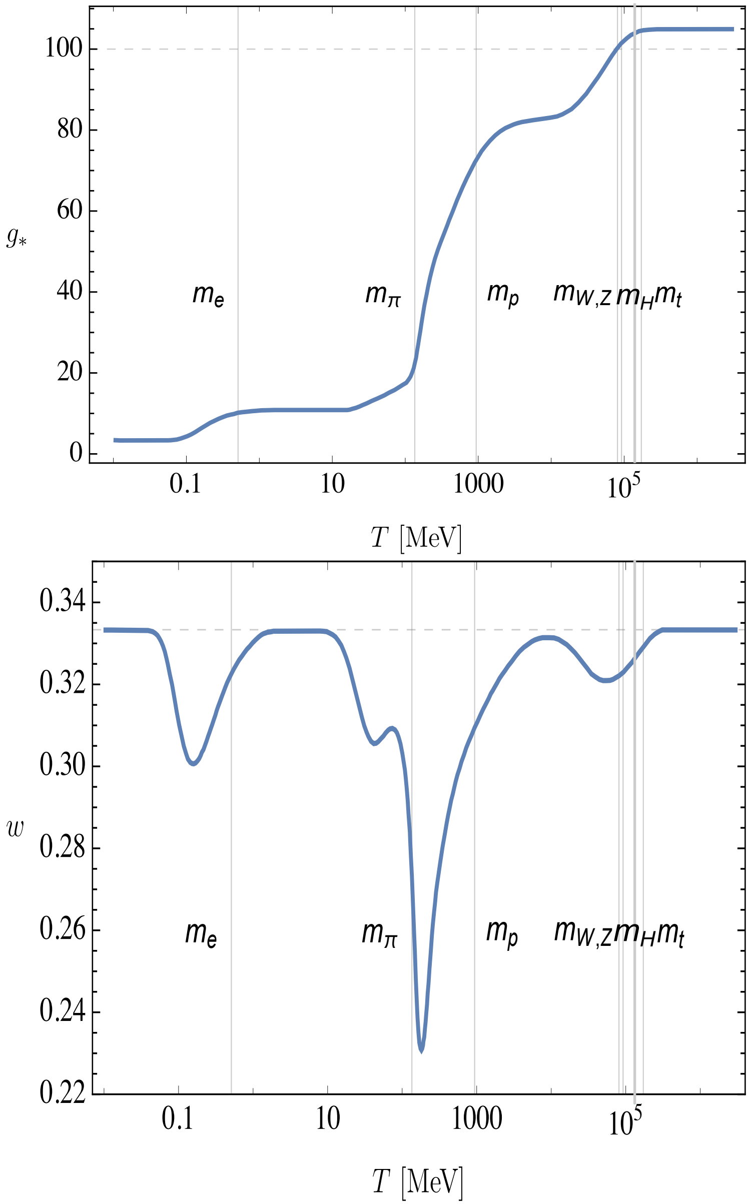

Carr, Clesse, JGB, Kühnel [1906.08217]

PBH mass spectrum

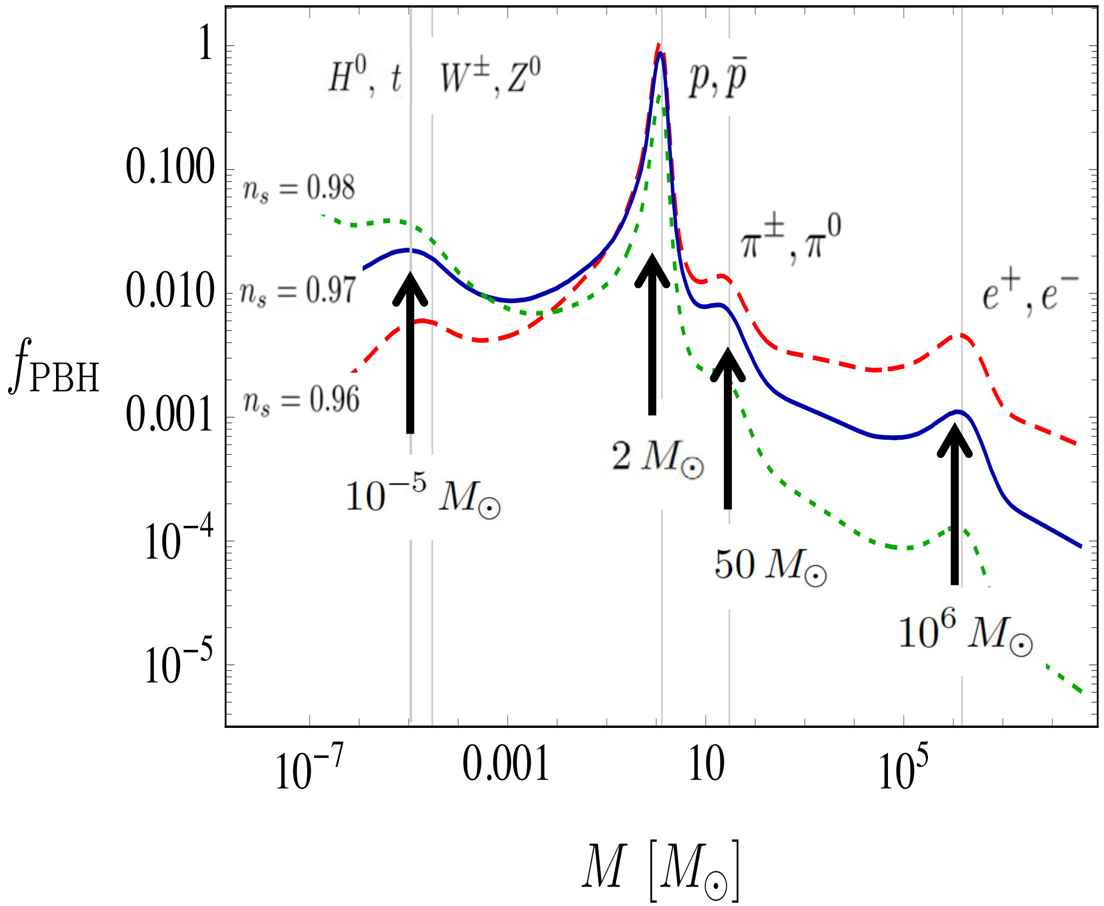

Spatial Distribution PBH

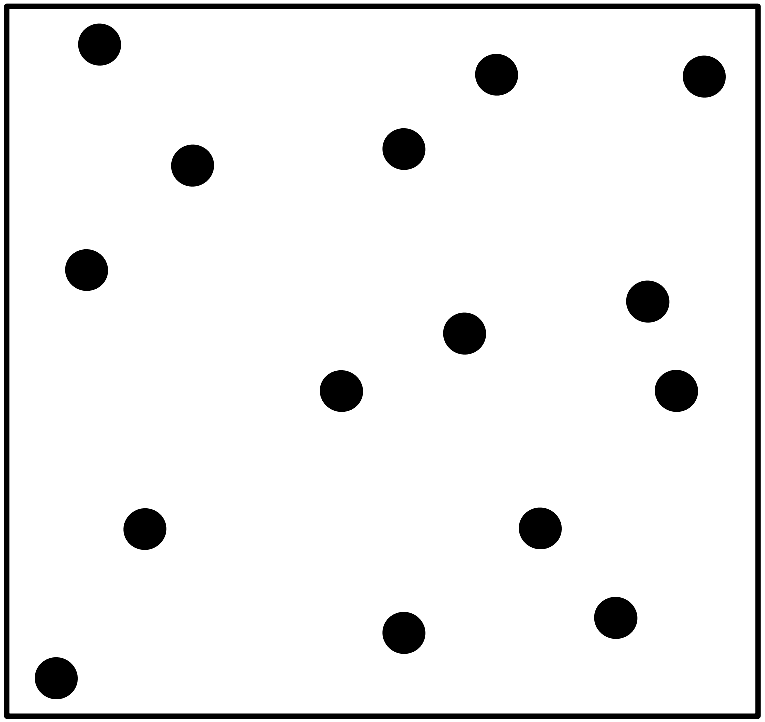

- Monochromatic
- Uniformly distributed

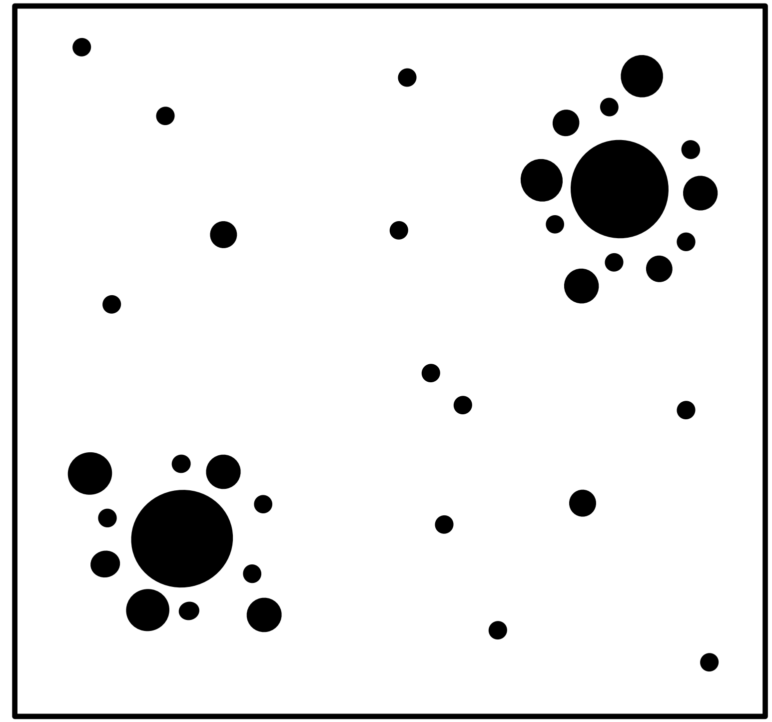

- Broad range of masses
- PBH in clusters

JGB [1702.08275]

Extended Mass Function of PBH

JGB, Clesse [1501.07565]

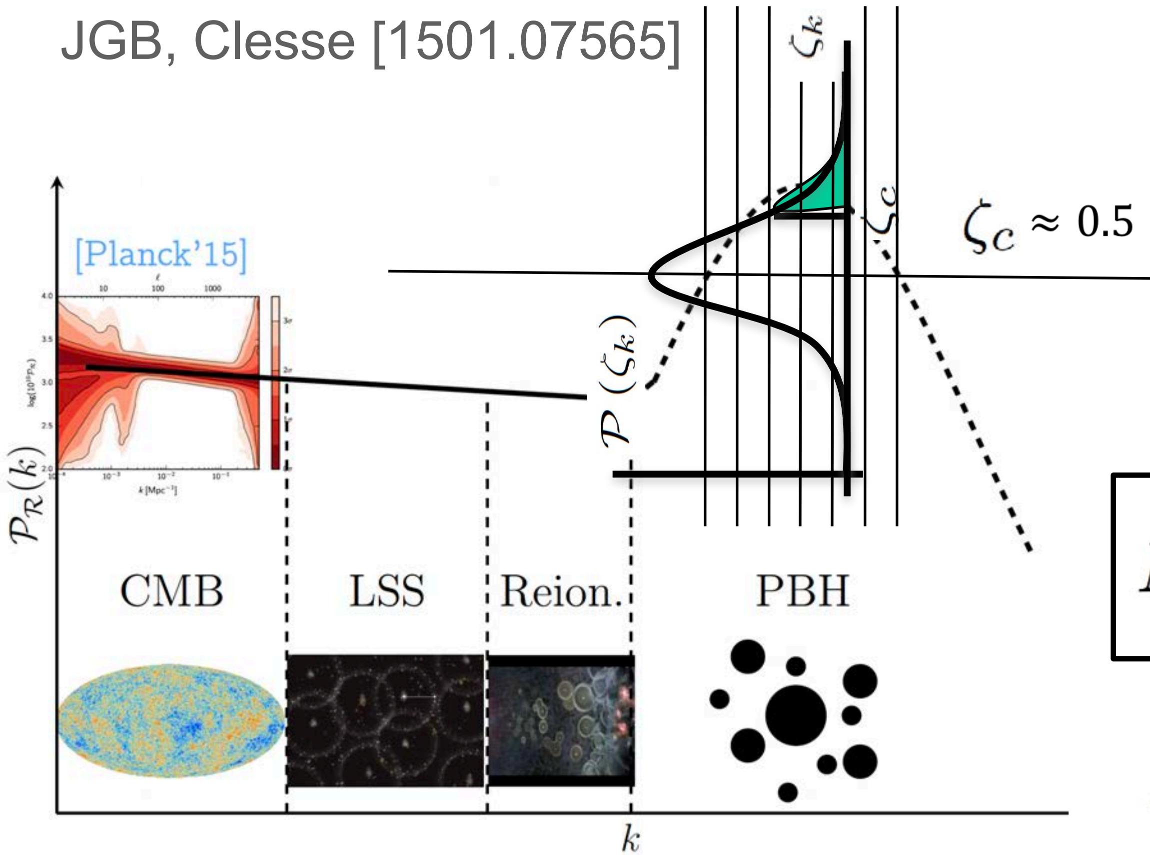

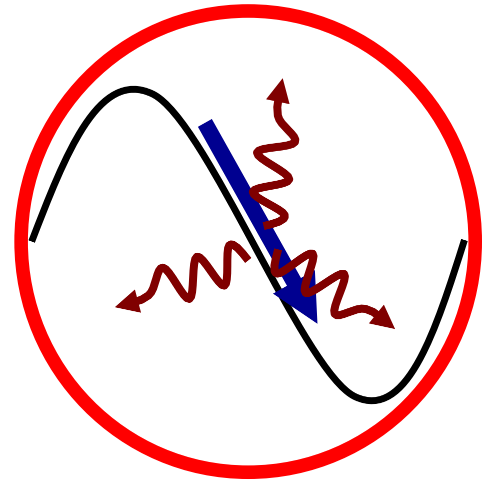

$$M_{\rm PBH} \simeq 30\, M_\odot\, e^{2(N-36)}$$

$$\beta^{\rm form}(M_k) = \int_{\zeta_c}^{\infty} \mathcal{P}(\zeta_k)\, d\zeta_k$$

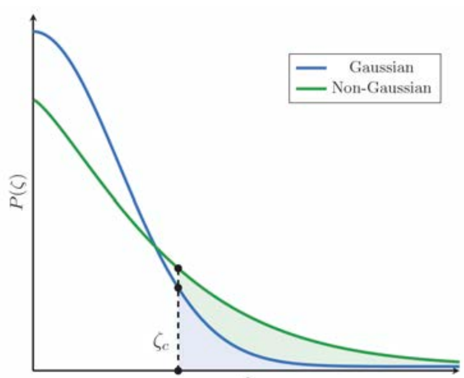

$$\beta(N) = \begin{cases} \mathrm{Erfc}\left(\dfrac{\zeta_c}{\sqrt{2P_\zeta(N)}}\right), & \text{Gaussian statistics}, \\ \mathrm{Erfc}\left(\sqrt{\dfrac{1}{2} + \dfrac{\zeta_c}{\sqrt{2P_\zeta(N)}}}\right), & \chi^2 \ \text{statistics} \end{cases}$$

Stochastic δN - formalism

Coarse-grained curvature perturbation

$$ds^2 = -dt^2 + a^2(t)e^{2\zeta(t,\mathbf{x})}\delta_{ij}dx^i dx^j \qquad \zeta_{\rm cg}(\mathbf{x}) = \delta N_{\rm cg}(\mathbf{x}) = \mathcal{N}(\mathbf{x}) - \langle\mathcal{N}\rangle$$

$$\frac{1}{M_{\rm pl}^2}\frac{d}{d\mathcal{N}}P_{\mathbf{\Phi}}(\mathcal{N}) = \left(-\sum_i \frac{v_{\phi_i}}{v}\frac{\partial}{\partial\phi_i} + v\sum_i \frac{\partial^2}{\partial\phi_i^2}\right)\cdot P_{\mathbf{\Phi}}(\mathcal{N})$$

Fokker-Planck Diffusion Eq.

Determined by the poles of the characteristic function

$$P_\phi(\mathcal{N}) = \frac{1}{2\pi}\int_{-\infty}^{\infty} e^{-it\mathcal{N}}\chi_{\mathcal{N}}(t,\phi)dt = \sum_n a_n(\phi)\,e^{-\Lambda_n\mathcal{N}}$$

Ezquiaga, JGB, Vennin [1912.05399]

$$\chi_{\mathcal{N}}(t,\phi) = \sum_n \frac{a_n(\phi)}{\Lambda_n - it} + \text{regular func}$$

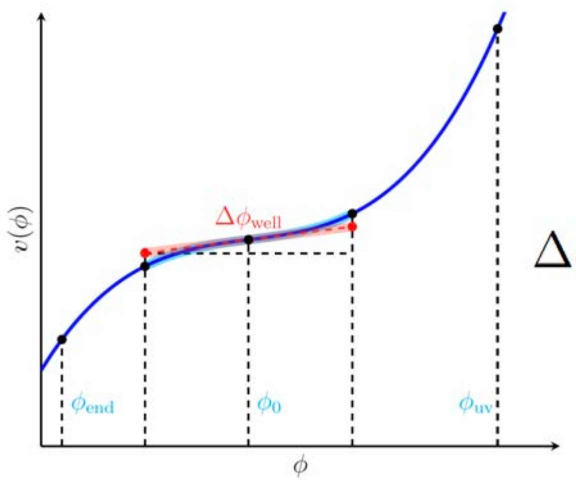

$$\alpha \gg (v_0^2\beta)^{1/3}$$

$$\Delta\phi_{\rm well} \simeq 2M_{\rm pl}\sqrt{\frac{\alpha}{3\beta}}$$

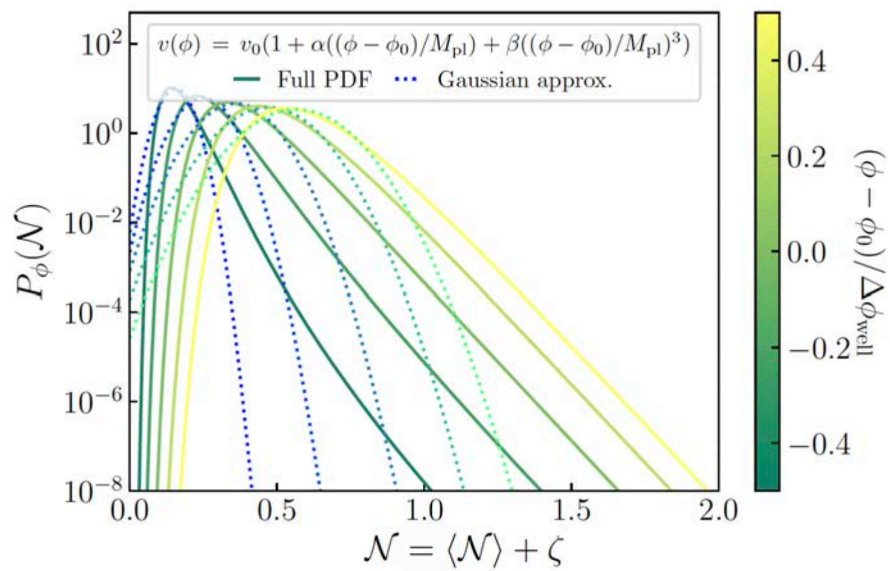

Quantum Diffusion @ CMB & LSS

Ezquiaga, JGB, Vennin [2207.06317]

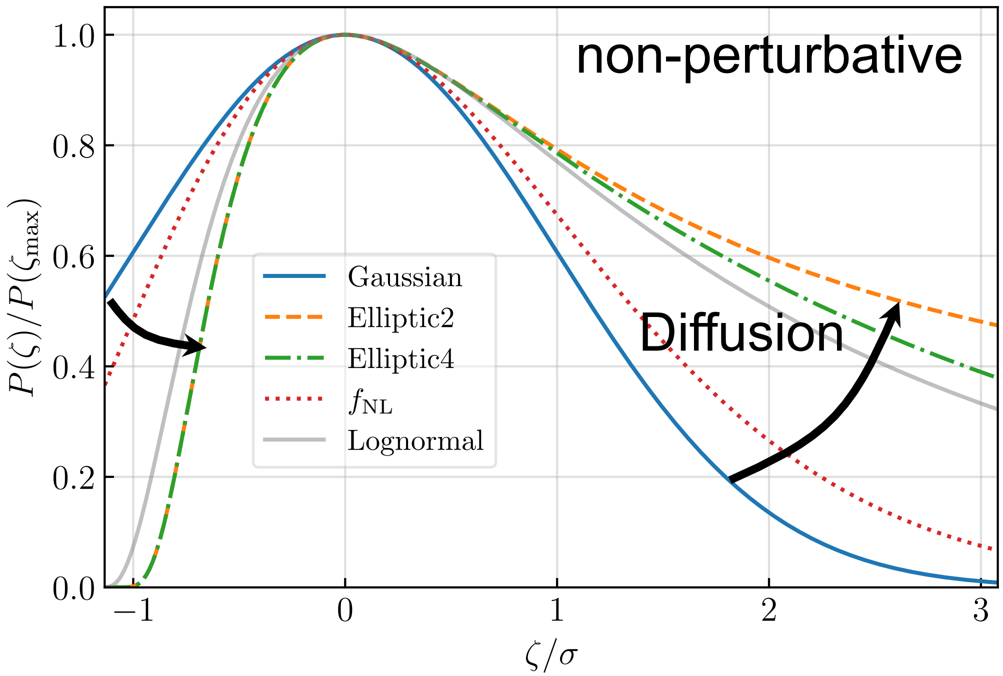

Elliptic Functions

$$P_2(\zeta_k) = -\frac{\pi}{2\mu^2}\vartheta_2'\left(\frac{\pi\alpha_k}{2}, e^{-\frac{\pi^2}{\mu^2}\mathcal{N}_k}\right)$$

$$P_4(\zeta_k) = \frac{\pi}{2\mu^2\alpha_k}\vartheta_4'\left(\frac{\pi\alpha_k}{2}, e^{-\frac{\pi^2}{\mu^2}\mathcal{N}_k}\right)$$

$f_{\rm NL}$ – expansion (not enough)

$$\zeta(x) = \zeta_{\rm G}(x) + \frac{3}{5} f_{\rm NL}\left[\zeta_{\rm G}^2(x) - \sigma_{\rm G}^2(x)\right]$$

$$P_{\rm NL}(\zeta) = \frac{1}{\sqrt{2\pi\sigma_{\rm G}^2\Delta}}\left[e^{-\frac{25(\sqrt{\Delta}-1)^2}{72 f_{\rm NL}^2\sigma_{\rm G}^2}} + e^{-\frac{25(\sqrt{\Delta}+1)^2}{72 f_{\rm NL}^2\sigma_{\rm G}^2}}\right]$$

$$\text{where} \quad \Delta(\zeta) = 1 + \frac{12}{5} f_{\rm NL}\zeta + \frac{36}{25} f_{\rm NL}^2\sigma_{\rm G}^2.$$

Lognormal distributions

$$\mathrm{LN}(x,\,\rho,\,\sigma) = \frac{1}{\rho\,\sigma\sqrt{2\pi}}\,\exp\left[-\frac{\ln(x/\rho)^2}{2\sigma^2} - \frac{\sigma^2}{2}\right]$$

$$\mathrm{G}(x,\,\rho,\,\sigma_{\rm G}) = \frac{1}{\sigma_{\rm G}\sqrt{2\pi}}\,\exp\left[-\frac{(x-\rho)^2}{2\sigma_{\rm G}^2}\right]$$

Quantum Diffusion @ CMB & LSS

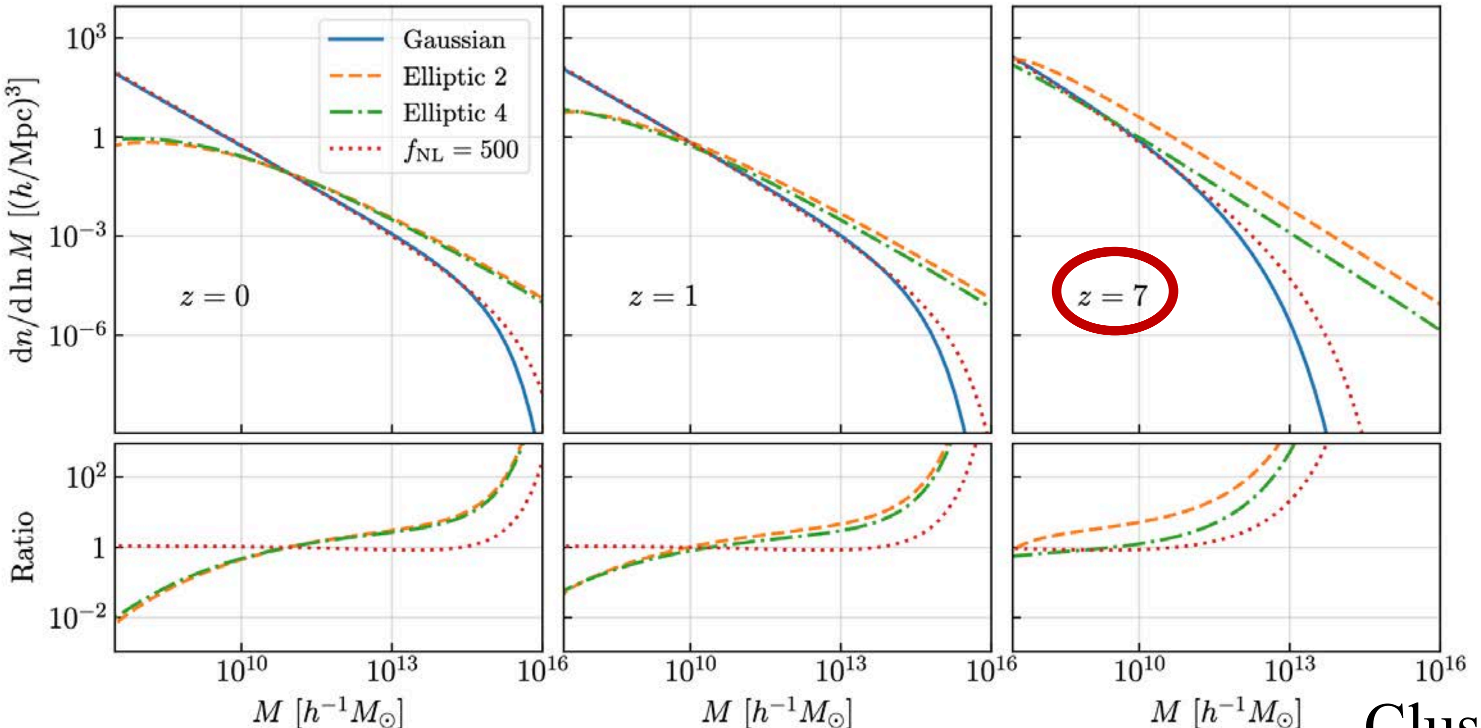

Halo Mass Function

Cluster Abundance

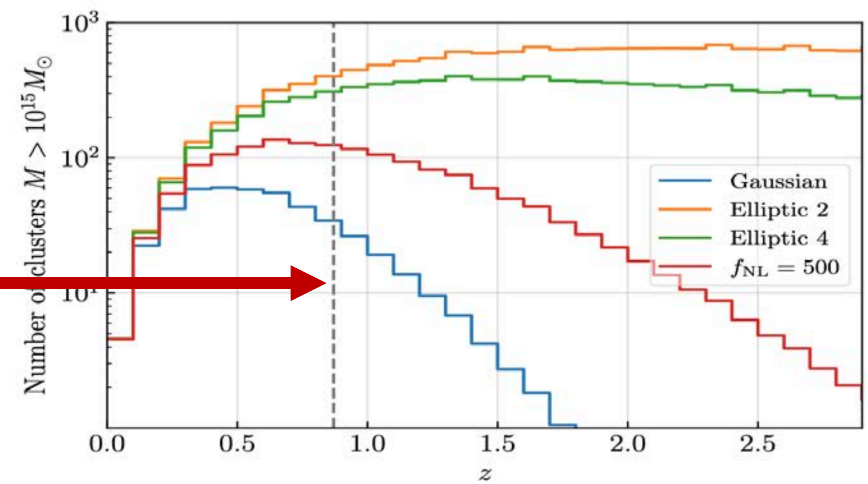

Ezquiaga, JGB, Vennin [2207.06317]

El Gordo

$$M \sim 3 \cdot 10^{15} M_\odot \text{ at } z = 0.87$$

Clustering from Quantum Diffusion

Animali, Vennin [2402.08642]

2-pt distribution function

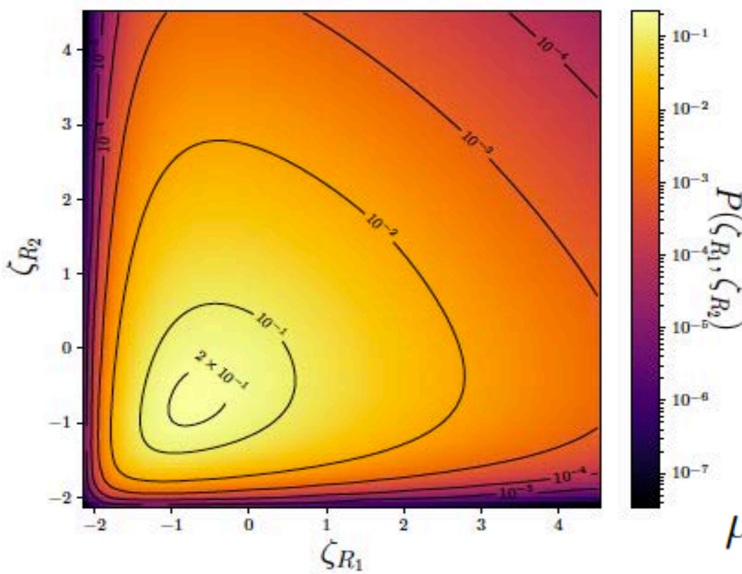

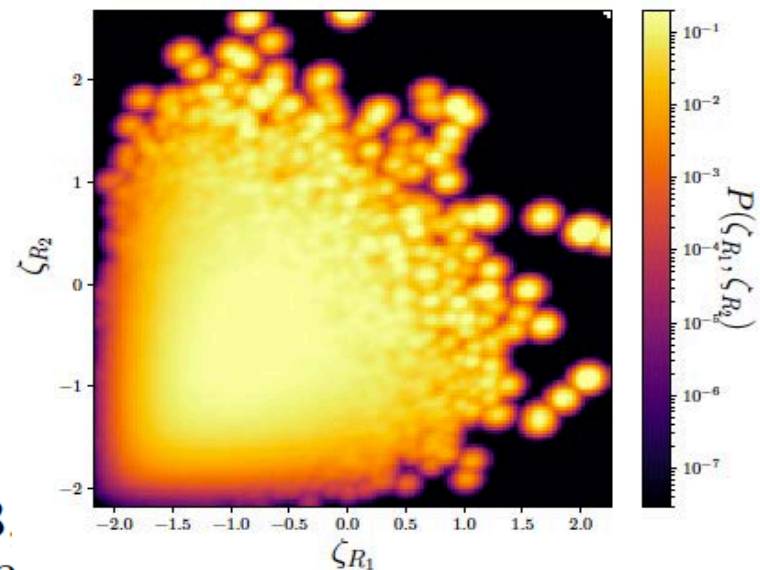

$\mu = 13.$

$d = 0.3$

Tilted-well potential

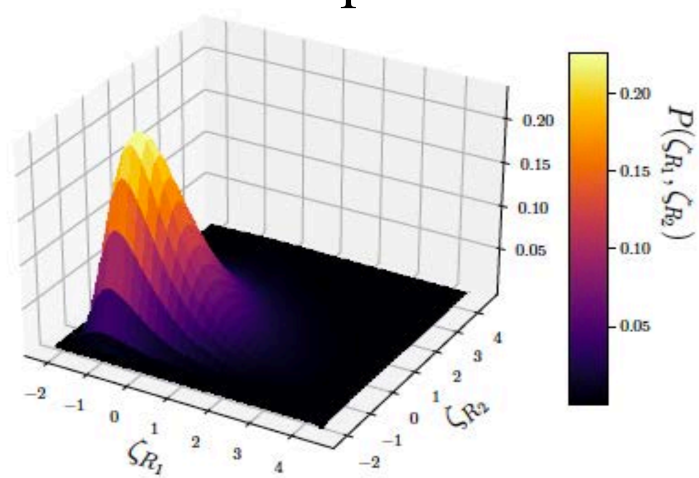

10^6 numerical simulations

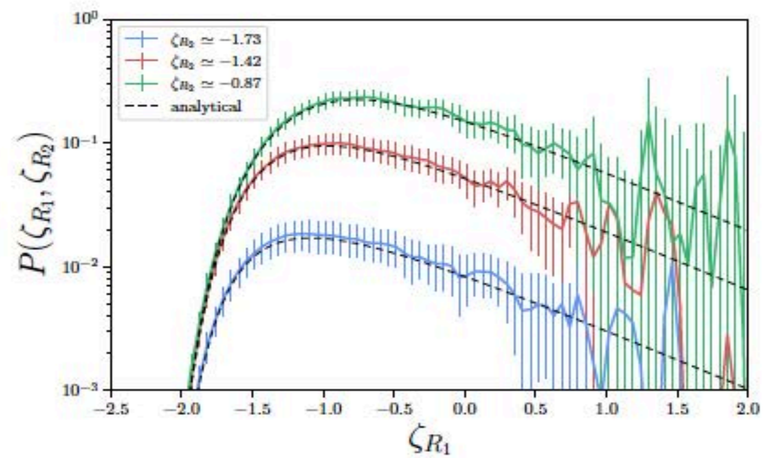

Clustering from Quantum Diffusion

2-pt distribution function

Animali, Vennin [2402.08642]

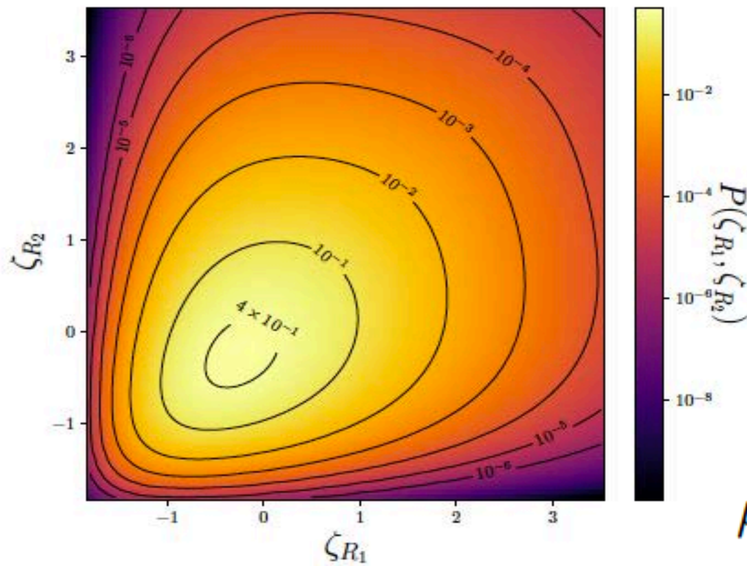

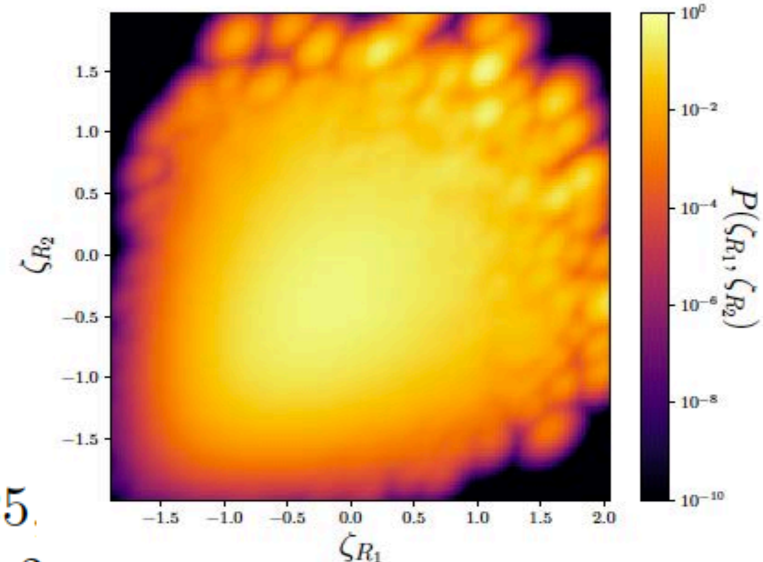

$\mu = 25.$

$d = 0.2.$

Tilted-well potential

10^6 numerical simulations

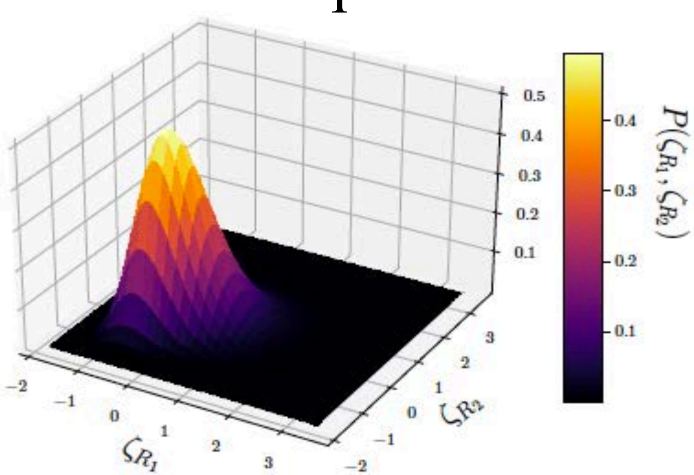

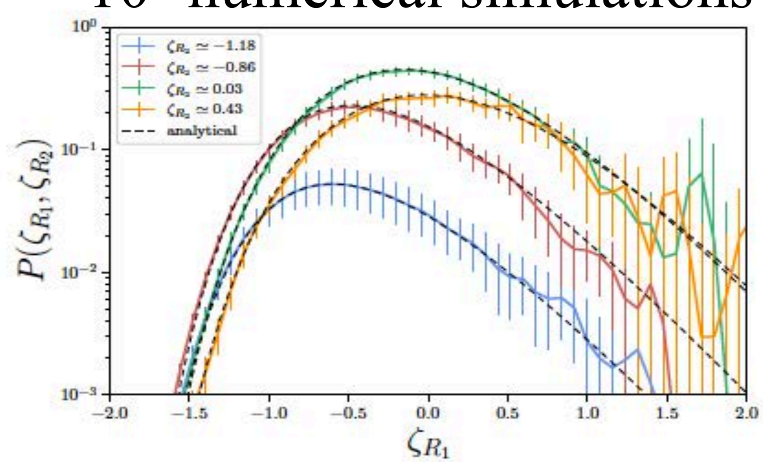

Observational Evidences

Observational evidence for primordial black holes

Carr, Clesse, JGB, Hawkins, Kühnel [2306.03903]

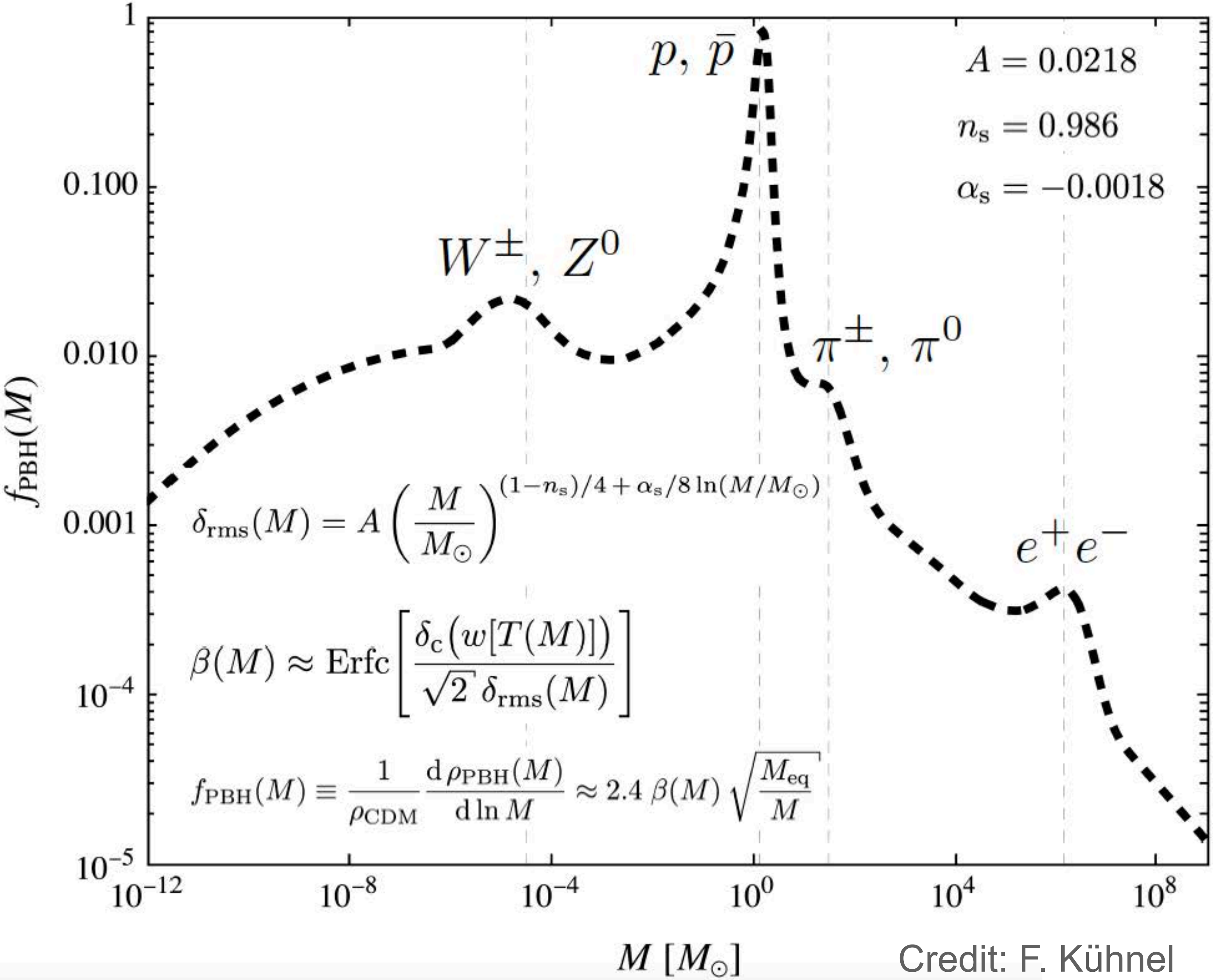

Credit: F. Kühnel

Observational evidence for primordial black holes

Carr, Clesse, JGB, Hawkins, Kühnel [2306.03903]

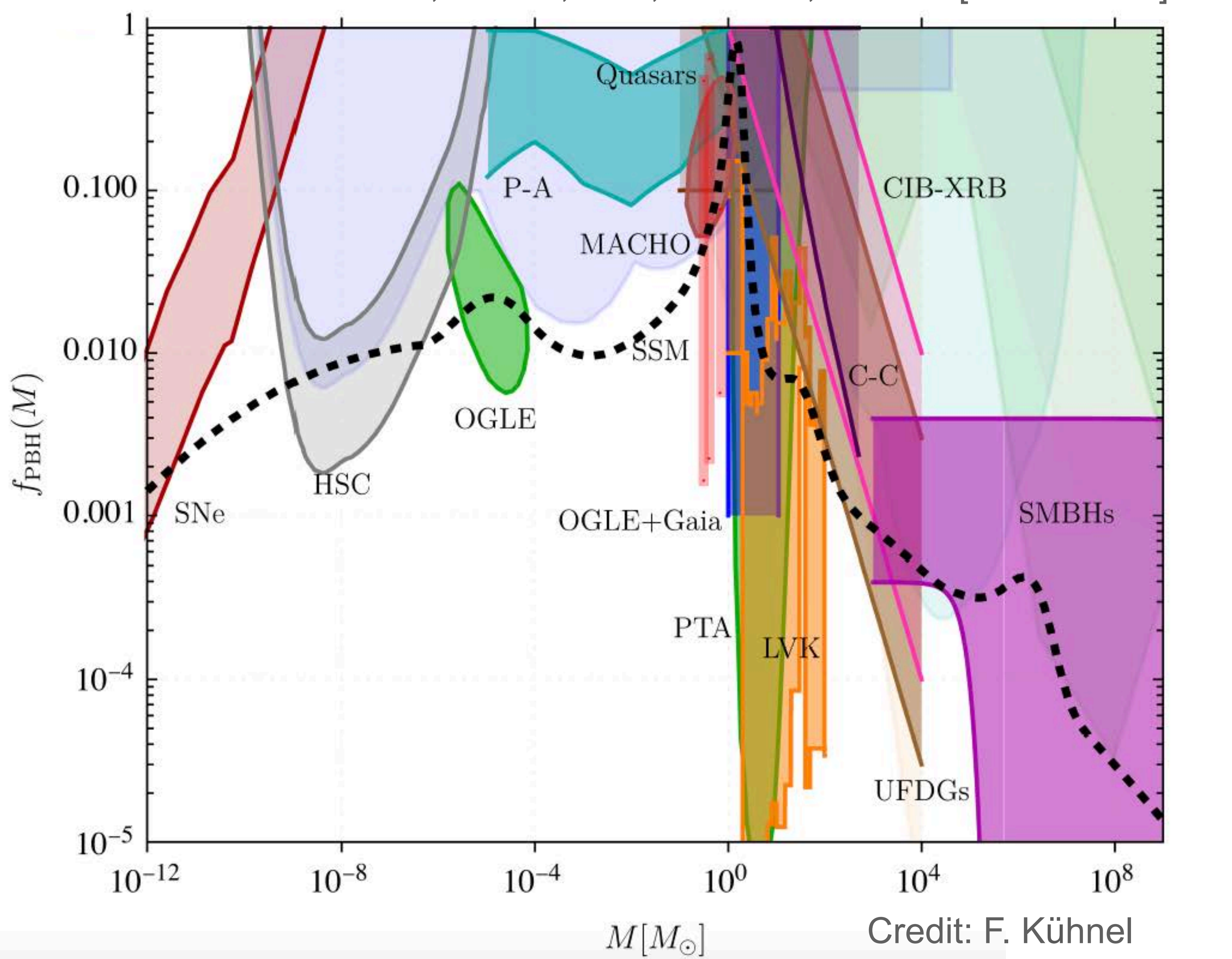

Credit: F. Kühnel

Observational evidence for primordial black holes

- Microlensing of Quasars
- MACHO events to LMC (Gaia DR3)
- Andromeda M31 pixel lensing
- OGLE+Gaia (solar-mass)
- OGLE+HSC (planetary-mass)
- MW ultra-high-velocity stars (Gaia DR2)
- MW tidal stream's perturbations
- UFDG min size
- UFDG mass-to-light ratio
- MW Disk heating
- Core-cusp in dwarf spheroidals
- SMBH seed accretion (JWST)
- high-z galaxies (HST/JWST)
- CIB - XRB source-subtracted correlations
- Radio background
- exploding white dwarfs SN (Goobar)
- SSM black hole candidates (LVK)
- LVK - GWTC-3 - (mass+spin+merger rates)
- PTAs – ISGW (Nanograv-IPTA)
- Dark Matter halos - rotation curves
- Matter-antimatter asymmetry

PBH could explain the SMBH in the center of galaxies seen by JWST at z ~ 13-16

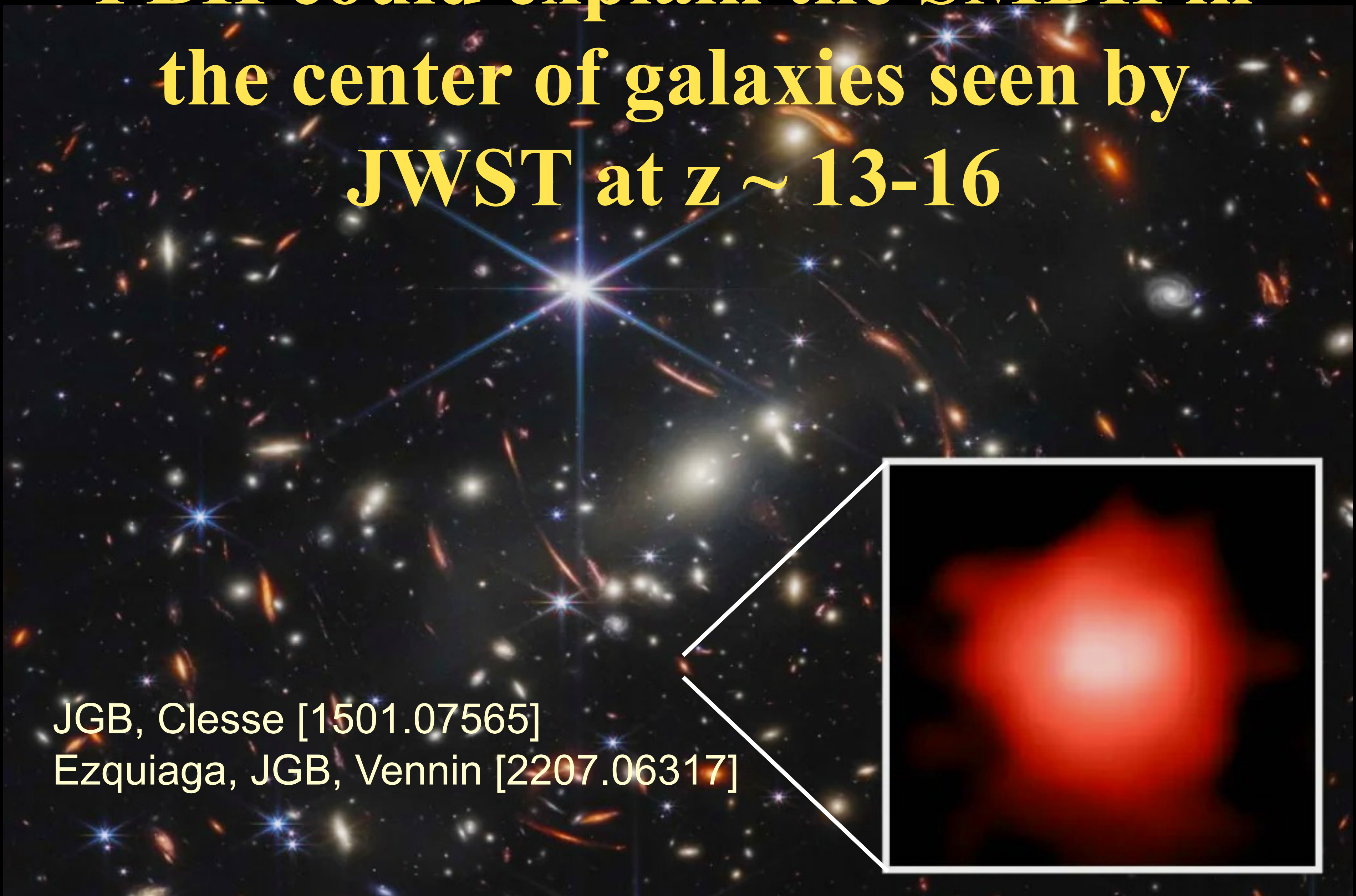

JGB, Clesse [1501.07565]
Ezquiaga, JGB, Vennin [2207.06317]

PBH could explain SMBH in AGN seen by JWST+Chandra at z ~ 10

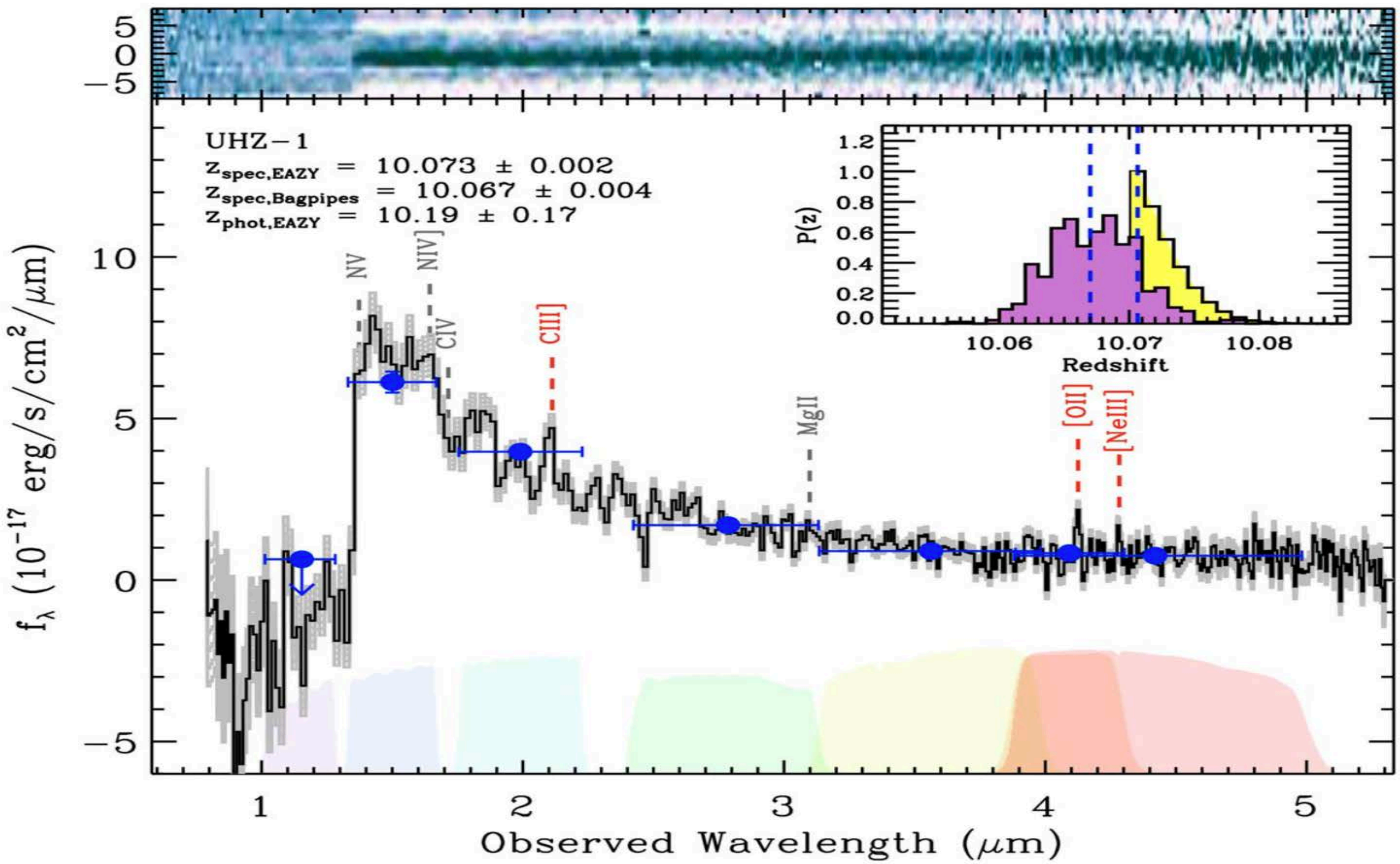

Figure 2. JWST/NIRSpec Prism spectroscopy of UHZ-1. Upper panel: 2D MSA Prism spectroscopy produced by msaexp. Lower panel: 1D spectral extraction in f_λ (in units of 10^{-17} erg s^{-1} cm^{-2} μm^{-1}) with associated statistical uncertainties (gray shaded region). Slit-loss corrections are defined by convolution of the JWST photometry with the Prism spectrum (see Section 2). Prominent and/or expected emission features are highlighted assuming $z_{\rm spec} = 10.07$ with significant $>3\sigma$ detections and nondetections labeled in red and gray, respectively. Overlaid are the JWST/NIRCam photometry (blue circles) with associated filter responses highlighted. Inset panel: redshift probability distributions for fits to the NIRSpec spectroscopy produced by EAZY (yellow) and BAGPIPES (purple) packages.

Cappelluti, Hasinger, Natarajan [2109.08701]

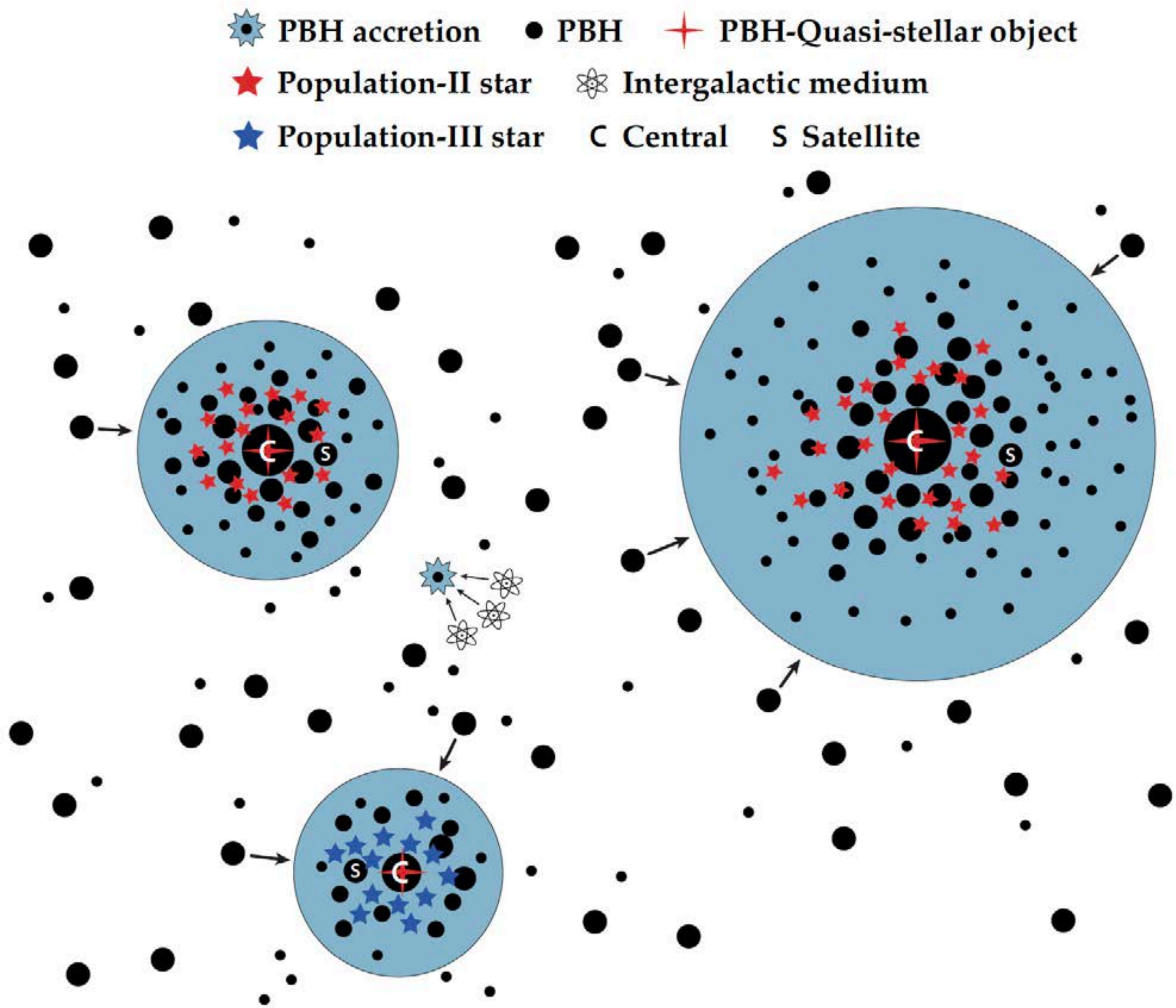

Figure 22. Illustration of PBH clustering at redshifts 10 – 15. Initially, PBHs (black dots) capture baryons while accreting, thereby contributing to the cosmic X-ray background. Lighter PBHs later form halos around more massive ones and initiate star formation; the lowest mass halos first form Population III stars, which generate a faint cosmic infrared background, and the higher mass ones then yield Population II stars. The most massive (central) supermassive PBH continues to accrete and merge with other PBHs. It appears as the central source in the infrared and X-ray emission, with the smaller PBHs and stars filling the halo as satellites.

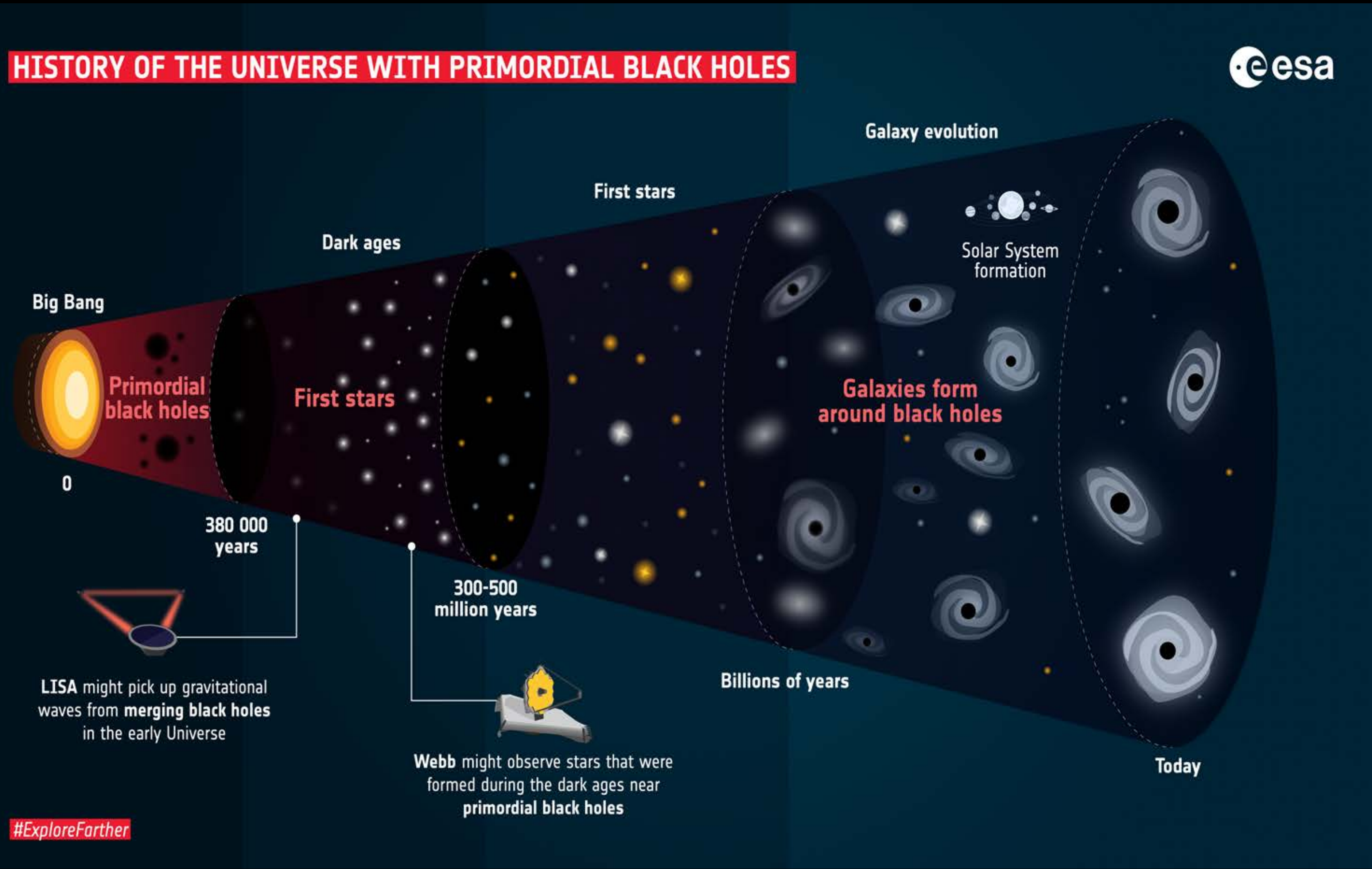
HISTORY OF THE UNIVERSE WITH PRIMORDIAL BLACK HOLES
esa
Big Bang
Primordial black holes
0
Dark ages
First stars
380 000 years
300-500 million years
First stars
Galaxy evolution
Solar System formation
Galaxies form around black holes
Billions of years
Today
LISA might pick up gravitational waves from merging black holes in the early Universe
Webb might observe stars that were formed during the dark ages near primordial black holes
#ExploreFarther

Microlensing

Microlensing

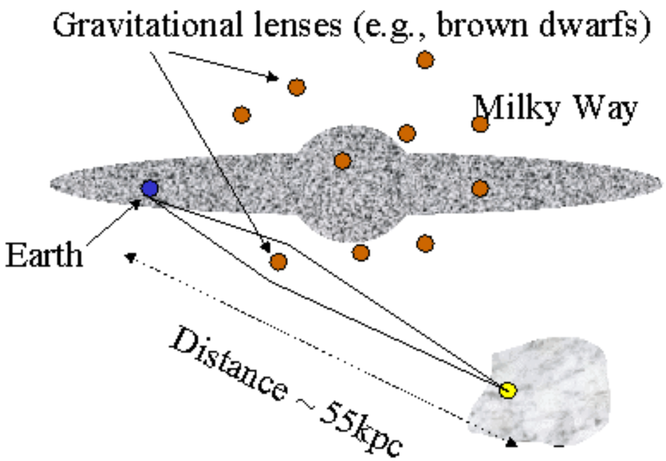

$$A = \frac{2+u^2}{u\sqrt{4+u^2}} \qquad u = \frac{r}{r_E} \quad \text{amplification}$$

$$\frac{1}{2}\,\overline{Dt} = \frac{r_E}{v} = \frac{\sqrt{4GM_D d}}{v} \quad \text{average crossing}$$

$$r_E^2 = 4GM_D\, d$$

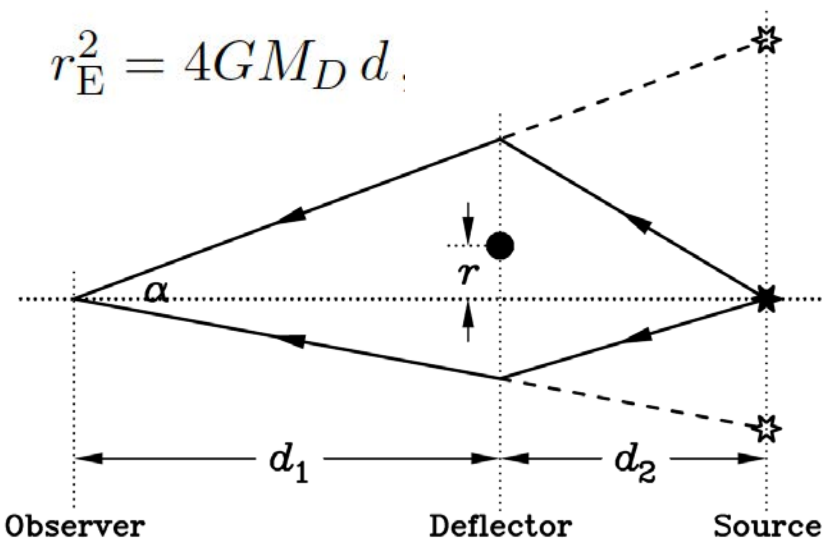

$$d = \frac{d_1 d_2}{d_1 + d_2}$$

$M_D = 100\,M_\odot$ => $\overline{Dt} = 4$ years

$M_D = 10\,M_\odot$ => $\overline{Dt} = 1.23$ years

$M_D = 1\,M_\odot$ => $\overline{Dt} = 5$ months

$M_D = 0.1\,M_\odot$ => $\overline{Dt} = 1.5$ months

$M_D = 0.01\,M_\odot$ => $\overline{Dt} = 2$ weeks

Credit: L. Wyrzykowski

OGLE3-UL-PAR-02 - candidate BH

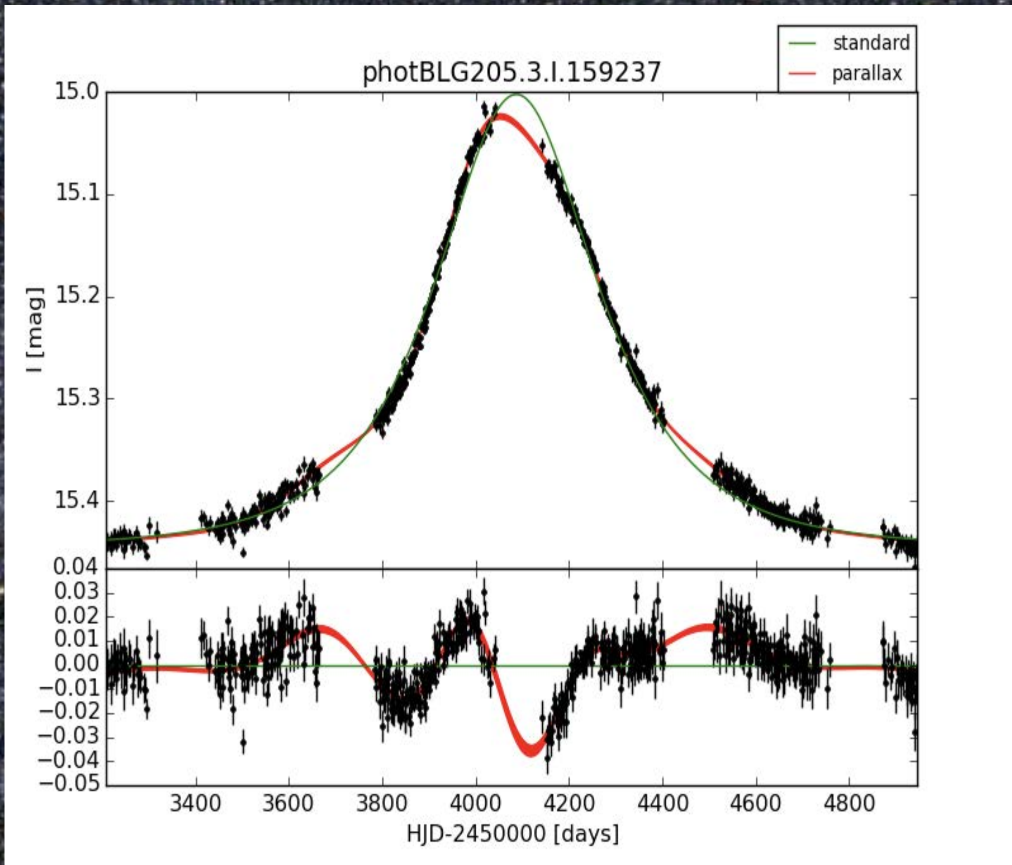

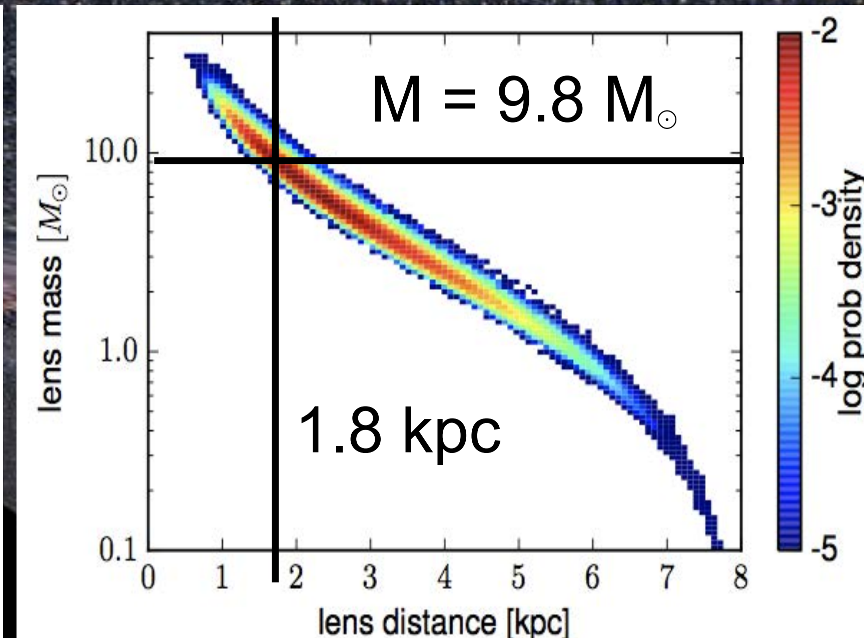

$$\frac{1}{2}\overline{Dt} = \frac{r_E}{v} = \frac{\sqrt{4GM_D d}}{v}$$

OGLE photometry
from 2001-2008
and microlensing model

Mass, Distance (degenerated estimate)

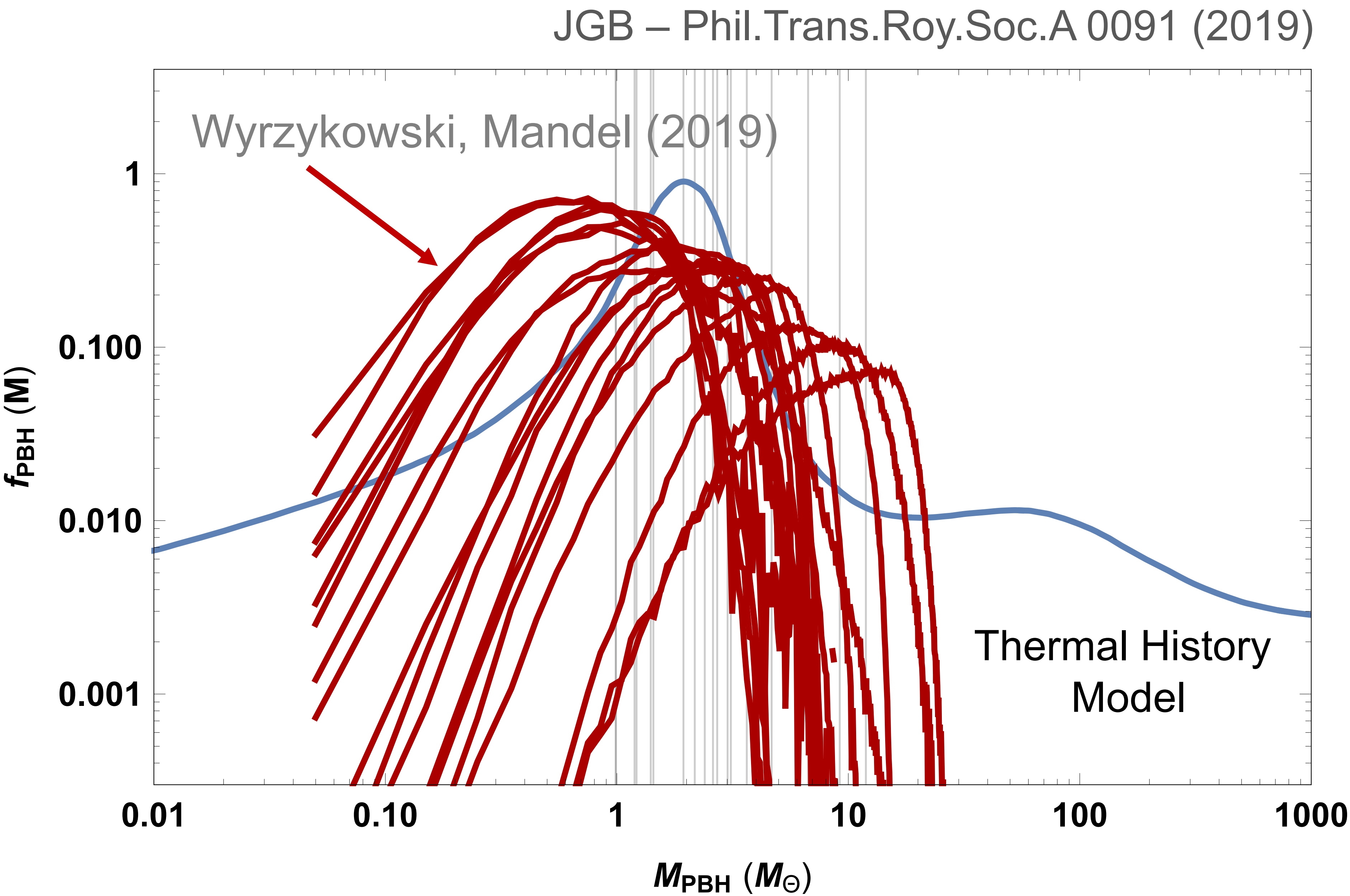

JGB – Phil.Trans.Roy.Soc.A 0091 (2019)
Wyrzykowski, Mandel (2019)
Thermal History
Model
1
0.100
0.010
0.001
f_{PBH} (M)
0.01
0.10
1
10
100
1000
M_{PBH} ($M_\odot$)

MW rotation curves

J. Jiao et al. (2023)
X. Ou et al. (2023)

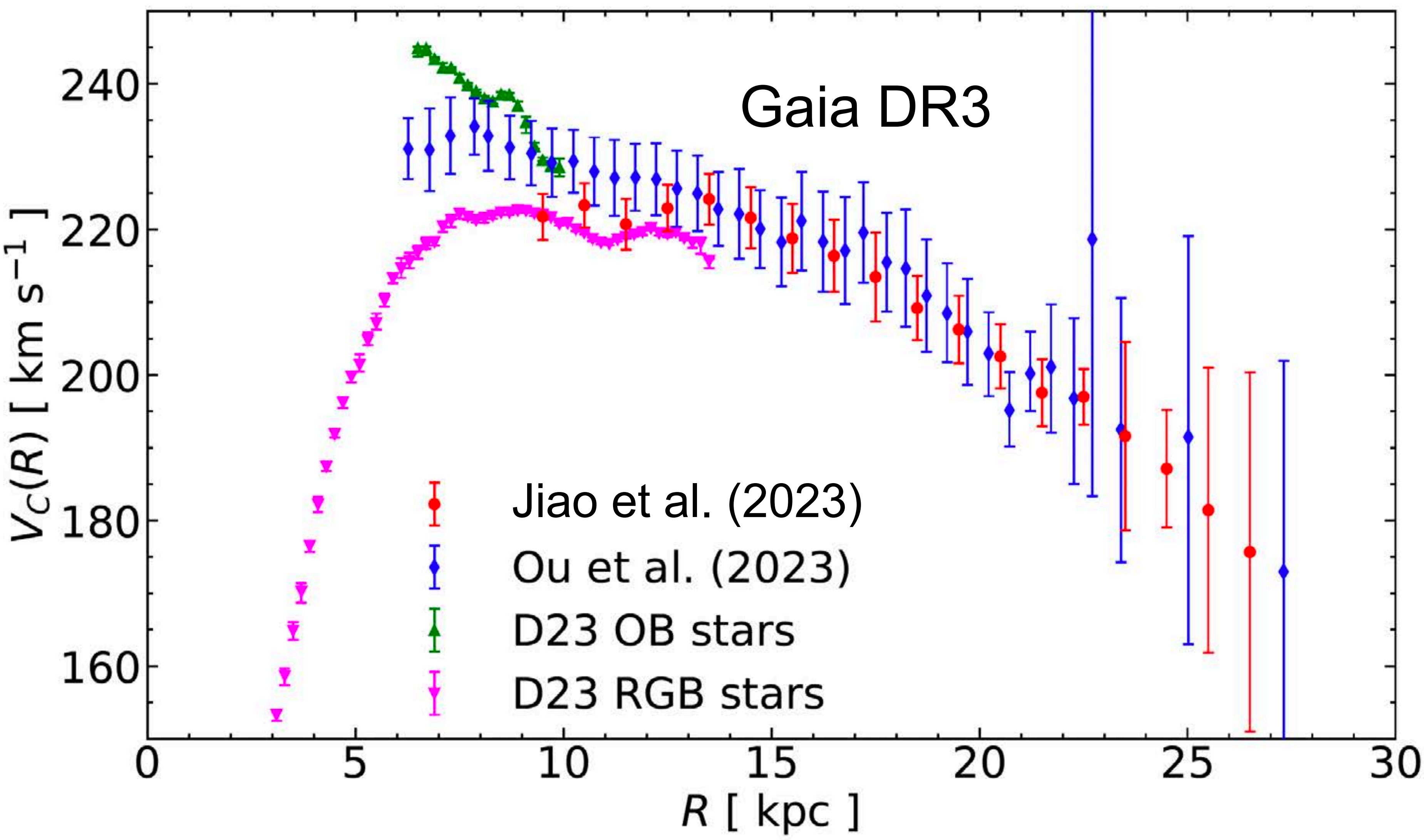

MW rotation curves

JGB, Hawkins [2402.00212]

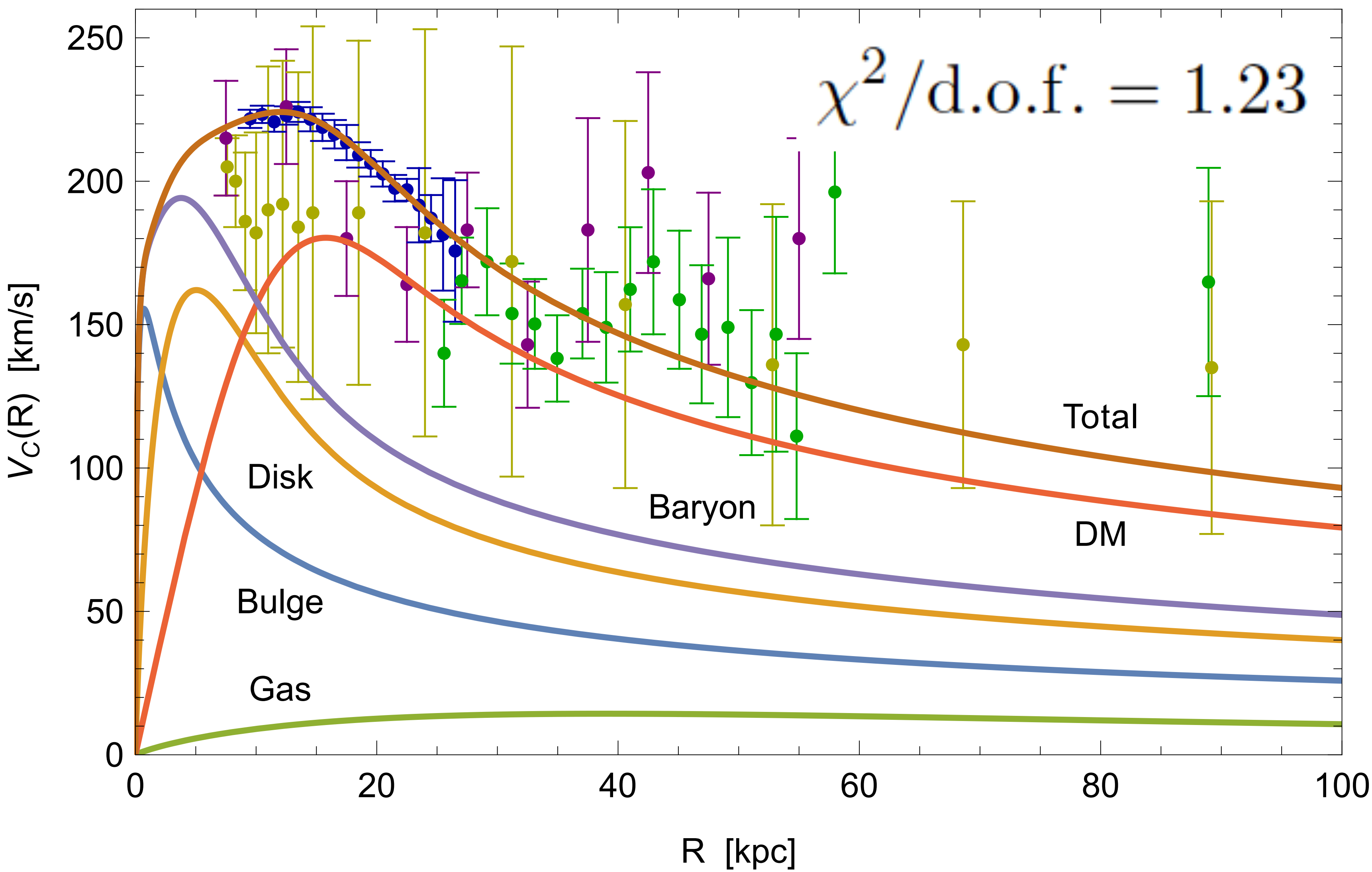

Optical depth

JGB, Hawkins [2402.00212]

$$r_E^2(x) = \frac{4GML}{c^2} \cdot x(1-x)$$

$$\tau = \frac{4\pi G L^2}{c^2} \int_0^1 \rho(R)\, x(1-x)\, dx$$

$$R \;=\; L\,(x_0^2 \,-\, 2x_0 x \cos b \cos l \,+\, x^2)^{1/2}$$

$$(b = -33^\circ,\; l = 280^\circ)$$

$$x_0 \;=\; R_\odot / L$$

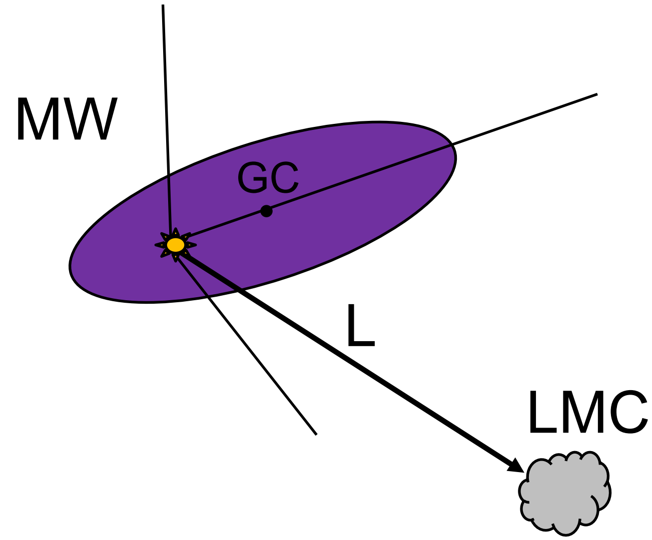

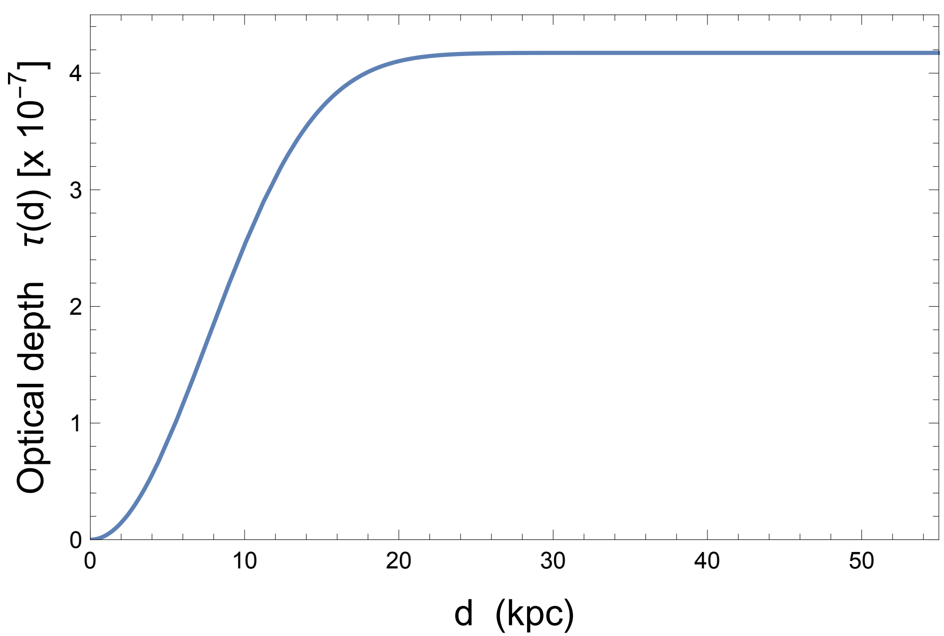

Expected No. events

JGB, Hawkins [2402.00212]

$$N_{\rm exp}(M) = E \int_0^\infty \frac{d\Gamma}{d\hat{t}}(M)\, \xi(\hat{t})\, d\hat{t}$$

MACHO survey $\quad E = 6.12 \times 10^7$ objects $\cdot$ years

EROS-2 survey $\quad E = 3.8 \times 10^7$ objects $\cdot$ years

$$\frac{d\Gamma}{d\hat{t}}(M) = \frac{32L}{\hat{t}^4 v_c^2 M} \int_0^1 \rho(R)\, r_E^4(x)\, \exp\left[-\frac{4r_E^2(x)}{\hat{t}^2 v_c^2}\right] dx$$

efficiency function $\xi(\hat{t})$

Efficiency Function

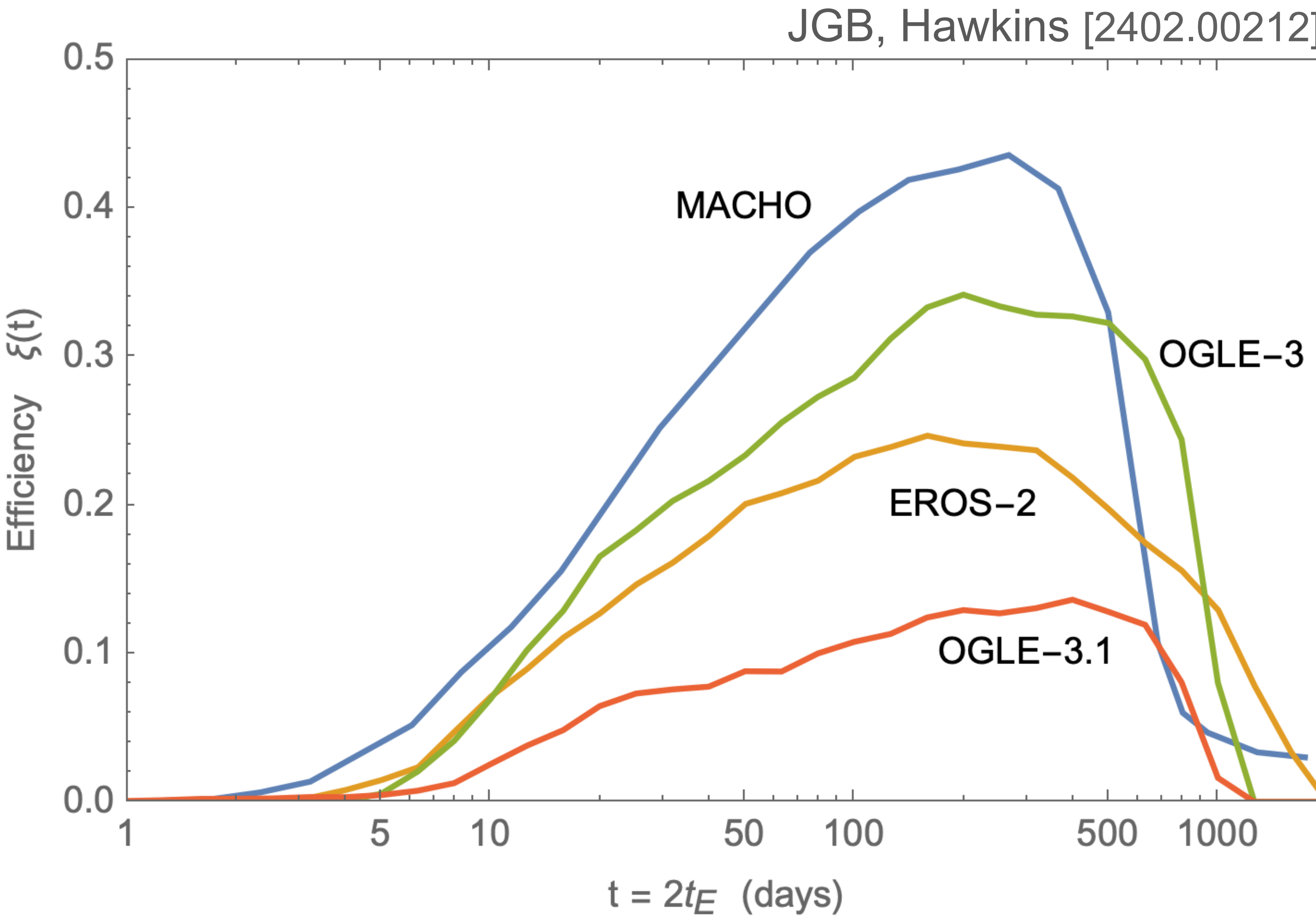

Microlensing Statistics

JGB, Hawkins [2402.00212]

the number of *observed* events is Poisson distributed

$$P(N_{\rm obs}) = \frac{e^{-N_{\rm avg}} N_{\rm avg}^{N_{\rm obs}}}{N_{\rm obs}!} = 0.05 \qquad N_{\rm obs} = z$$

$$N_{\rm avg} \le N^*_{\rm avg} \simeq 3 + \ln\left(\frac{N_*^z}{z!}\right) \simeq 3 + 1.3\,z - 0.01\,z^2$$

95% confident (2σ)

$$N^*_{\rm avg} \simeq 5.9 + 1.74z - 0.017z^2$$

99.73% confidence (3σ)

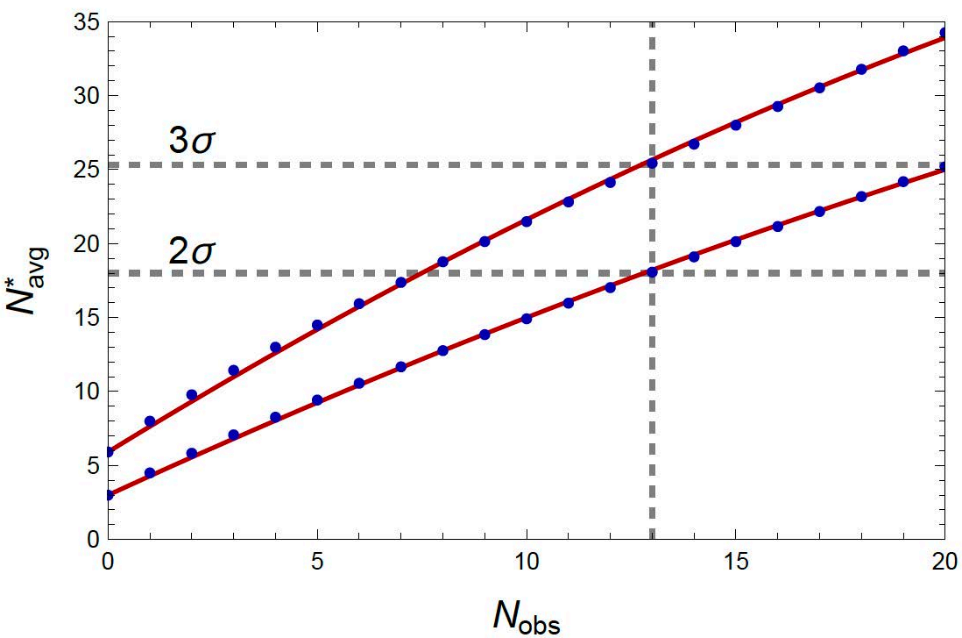

Constraints

JGB, Hawkins [2402.00212]

$$C(M) = \frac{N_{\rm avg}}{N_{\rm exp}(M)} \leq \frac{N^*_{\rm avg}}{N_{\rm exp}(M)} \qquad \text{monochromatic}$$

extended mass distribution

$$\int_0^\infty \frac{dM}{M} f(M) N_{\rm exp}(M) \leq N^*_{\rm avg}$$

$$\int_0^\infty \frac{dM}{M} f(M) = f_{\rm PBH} \qquad \text{normalized}$$

$$f_{\rm PBH} \leq \left[\int_0^\infty \frac{dM}{M} \frac{f(M)}{C(M)} \right]^{-1}$$

PBH Constraints

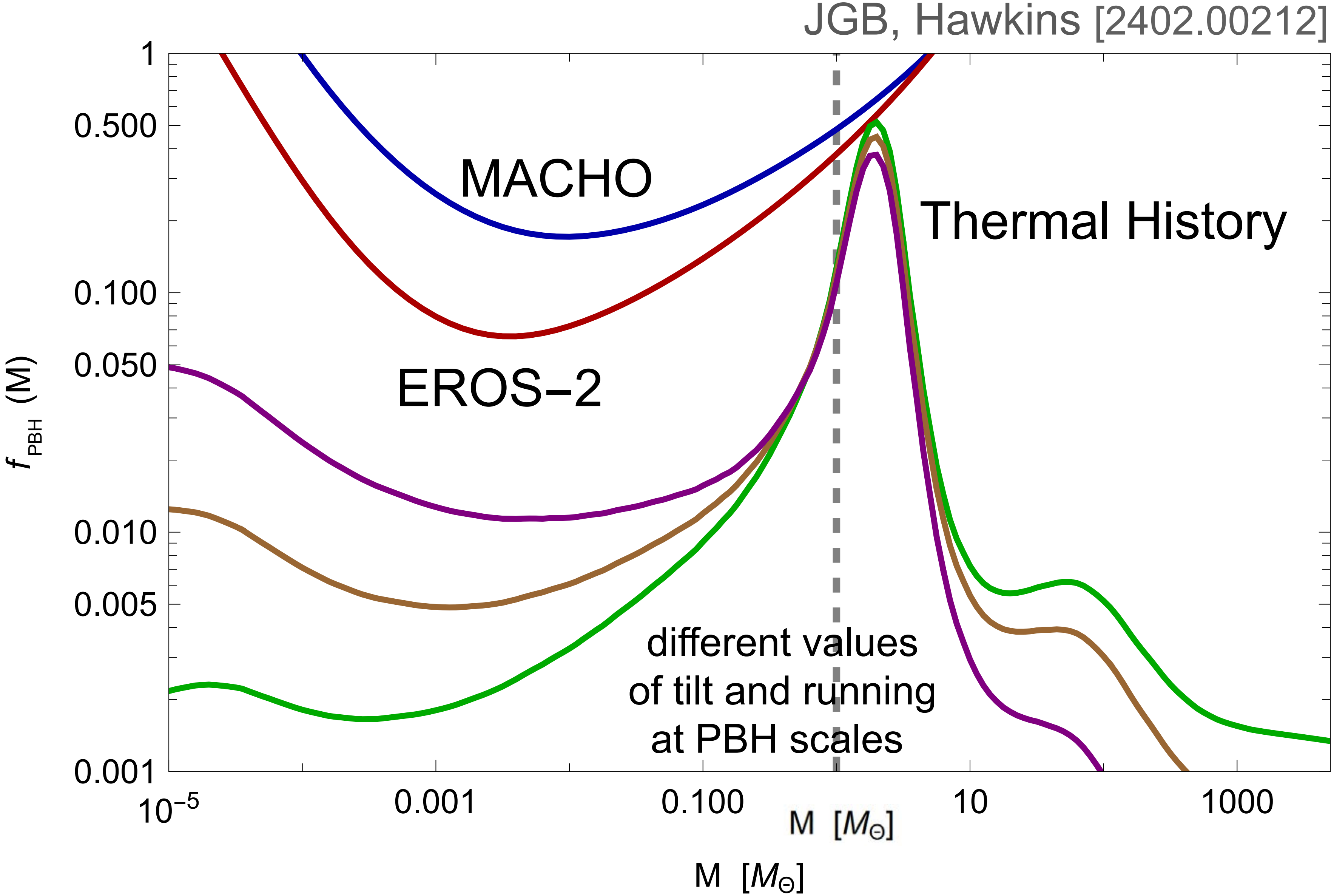

Halo Mass Fraction

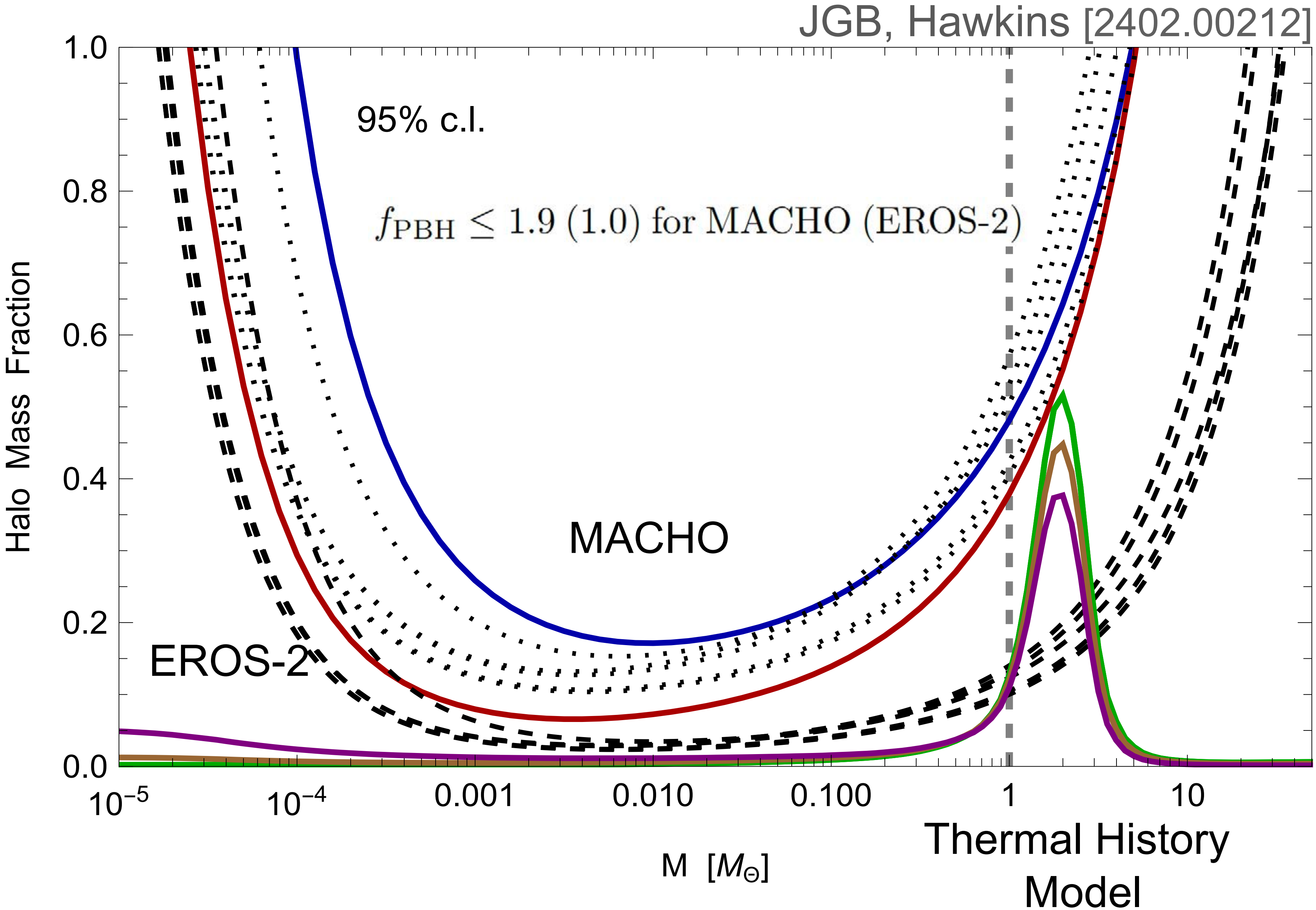

PBH could be all of the DM

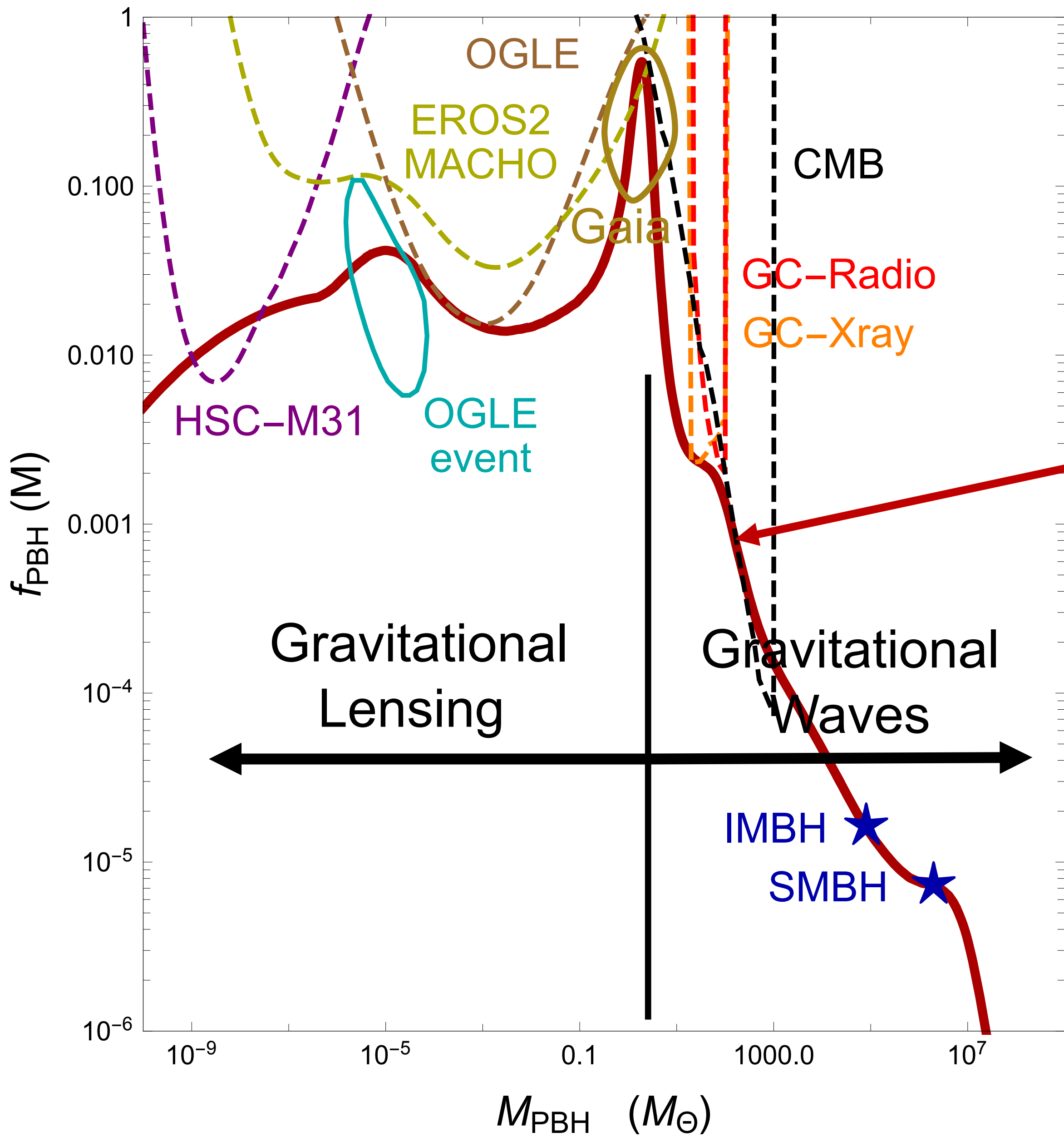

Cappelluti
Hasinger
Natarajan
(2022)

JGB
Private
communication

Gravitational Waves

GWTC-3 LVK Coll. (2022)

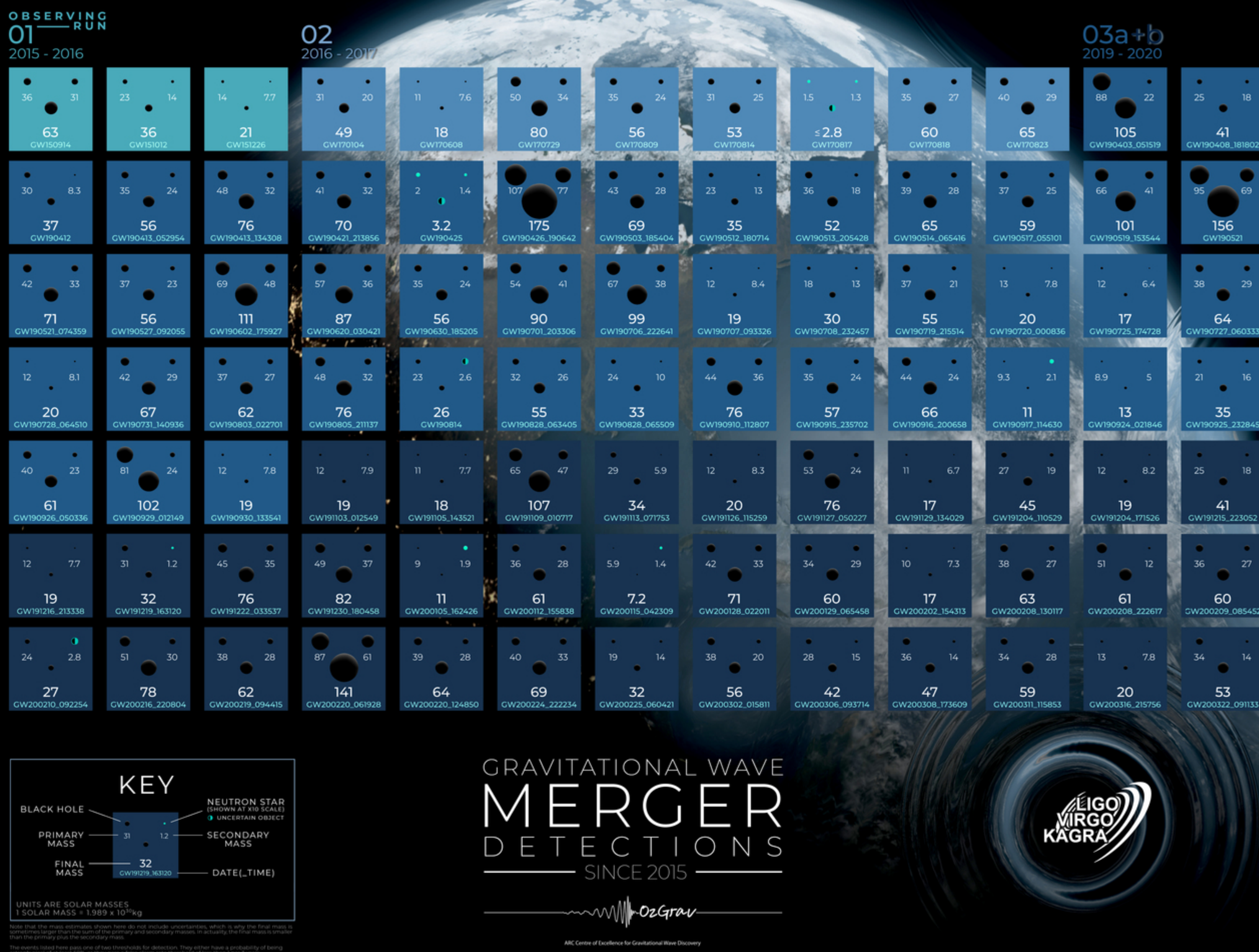

Black Holes and Neutron Stars

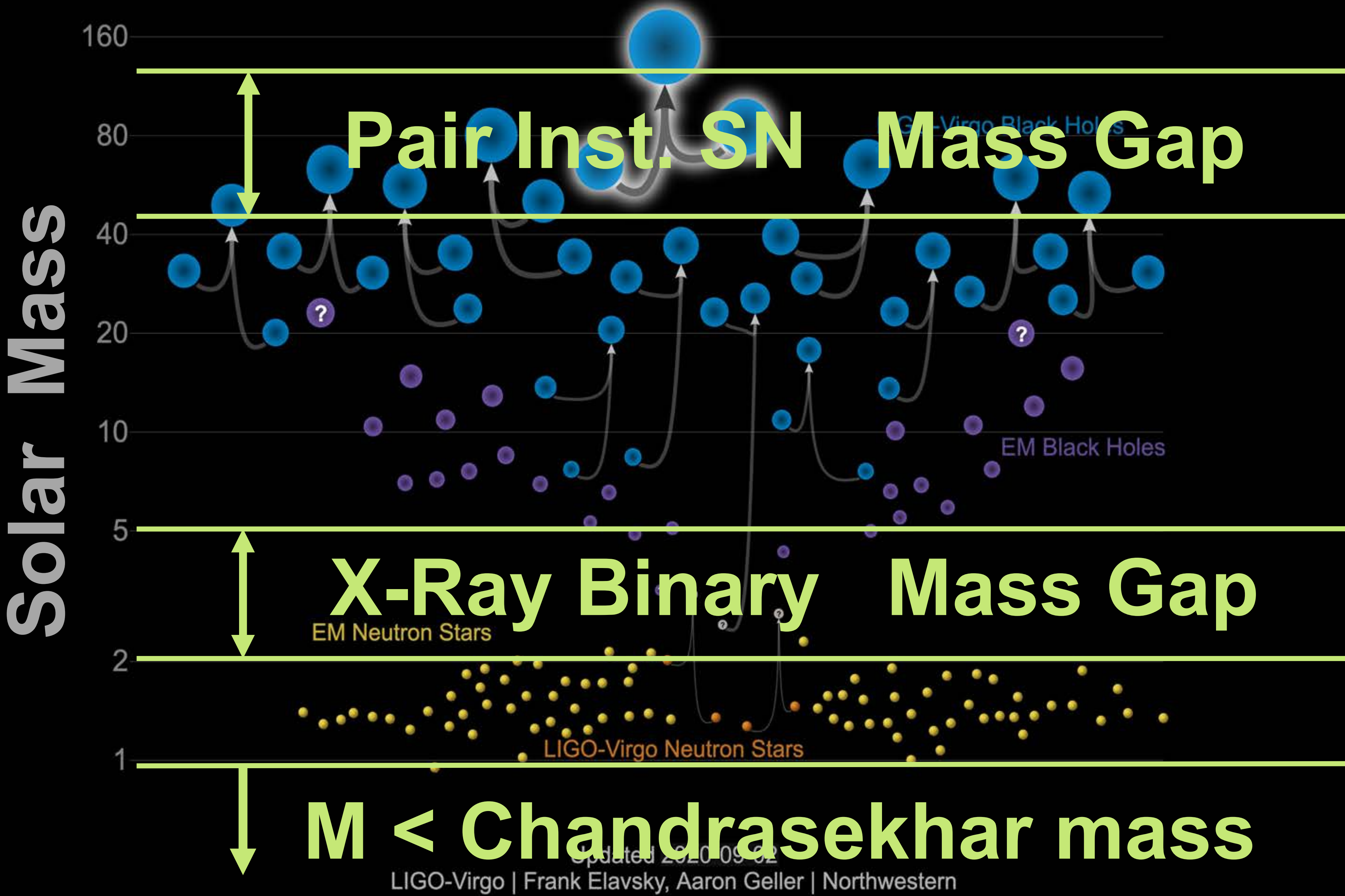

Primary and secondary masses

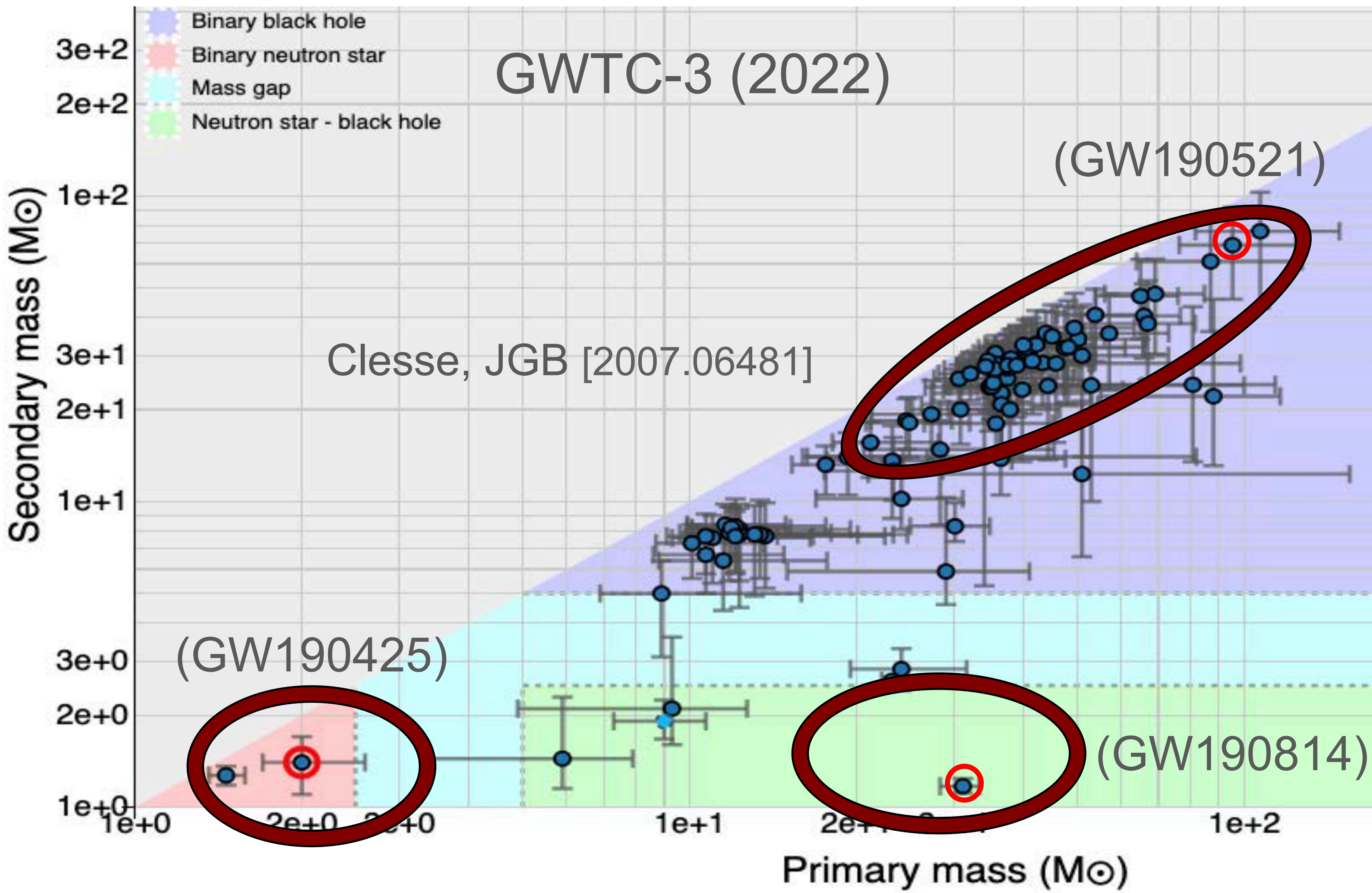

Are LIGO/Virgo BH Primordial?

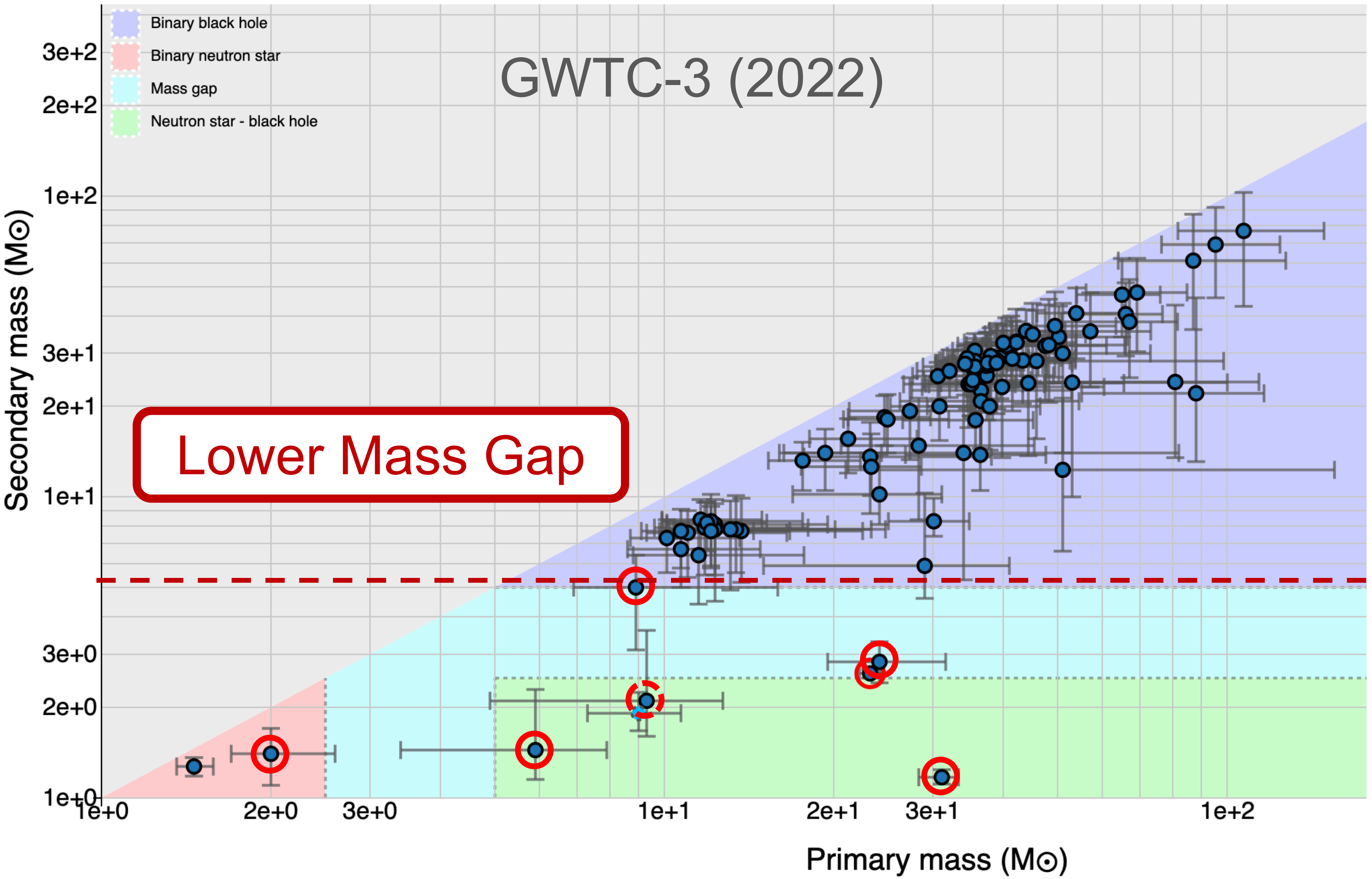

Are LIGO/Virgo BH Primordial?

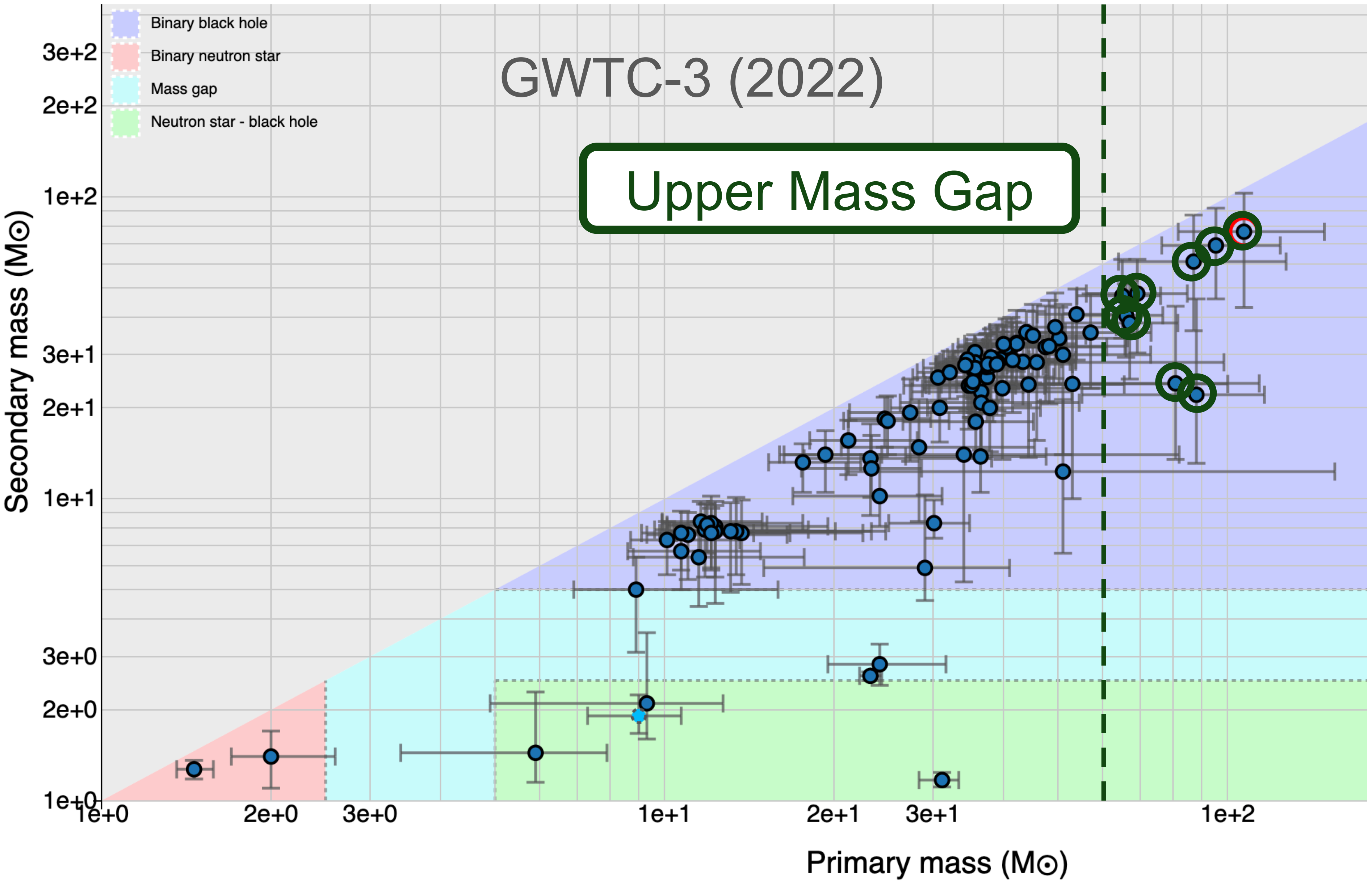

Are LIGO/Virgo BH Primordial?

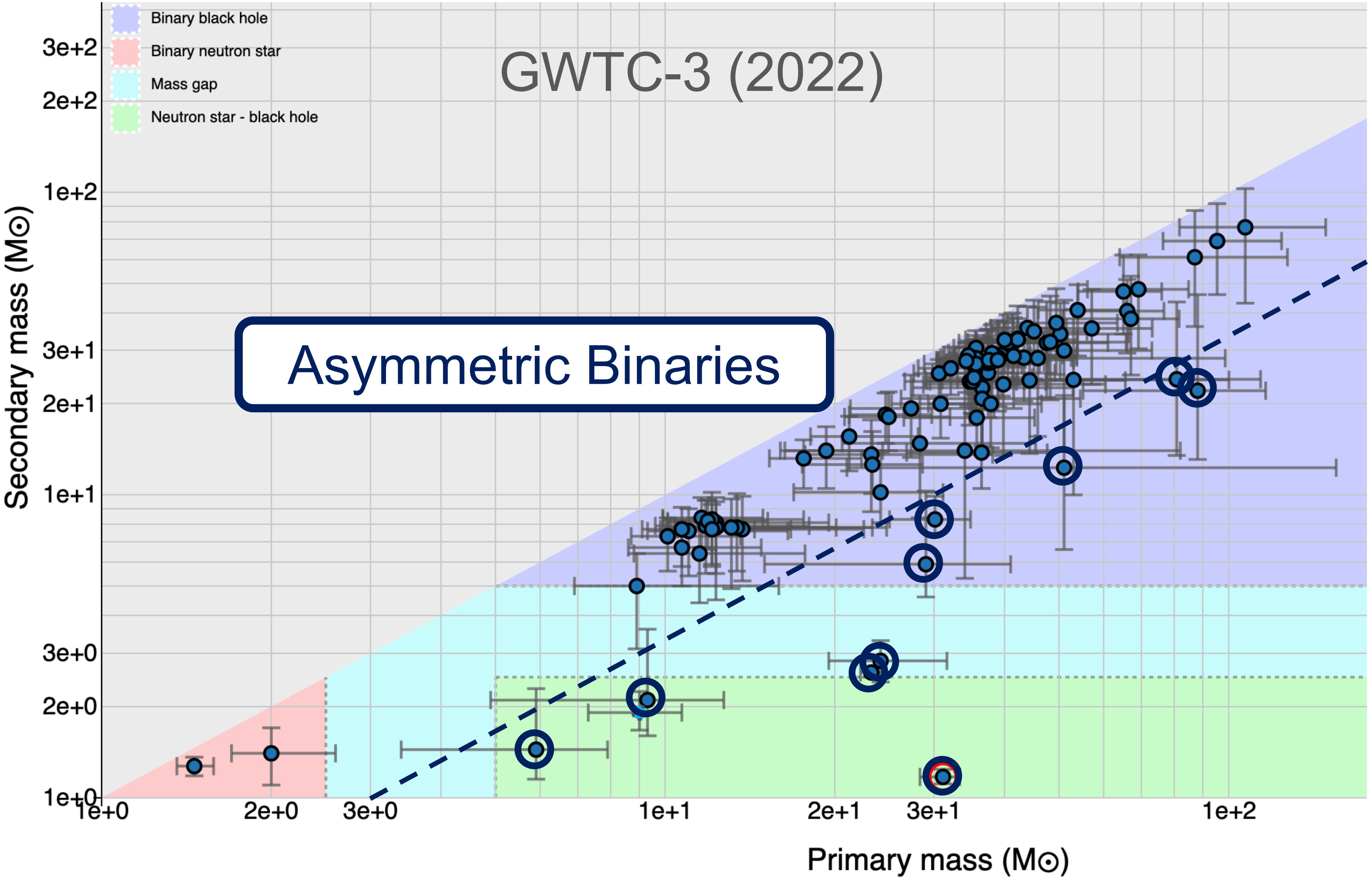

Are LIGO/Virgo BH Primordial?

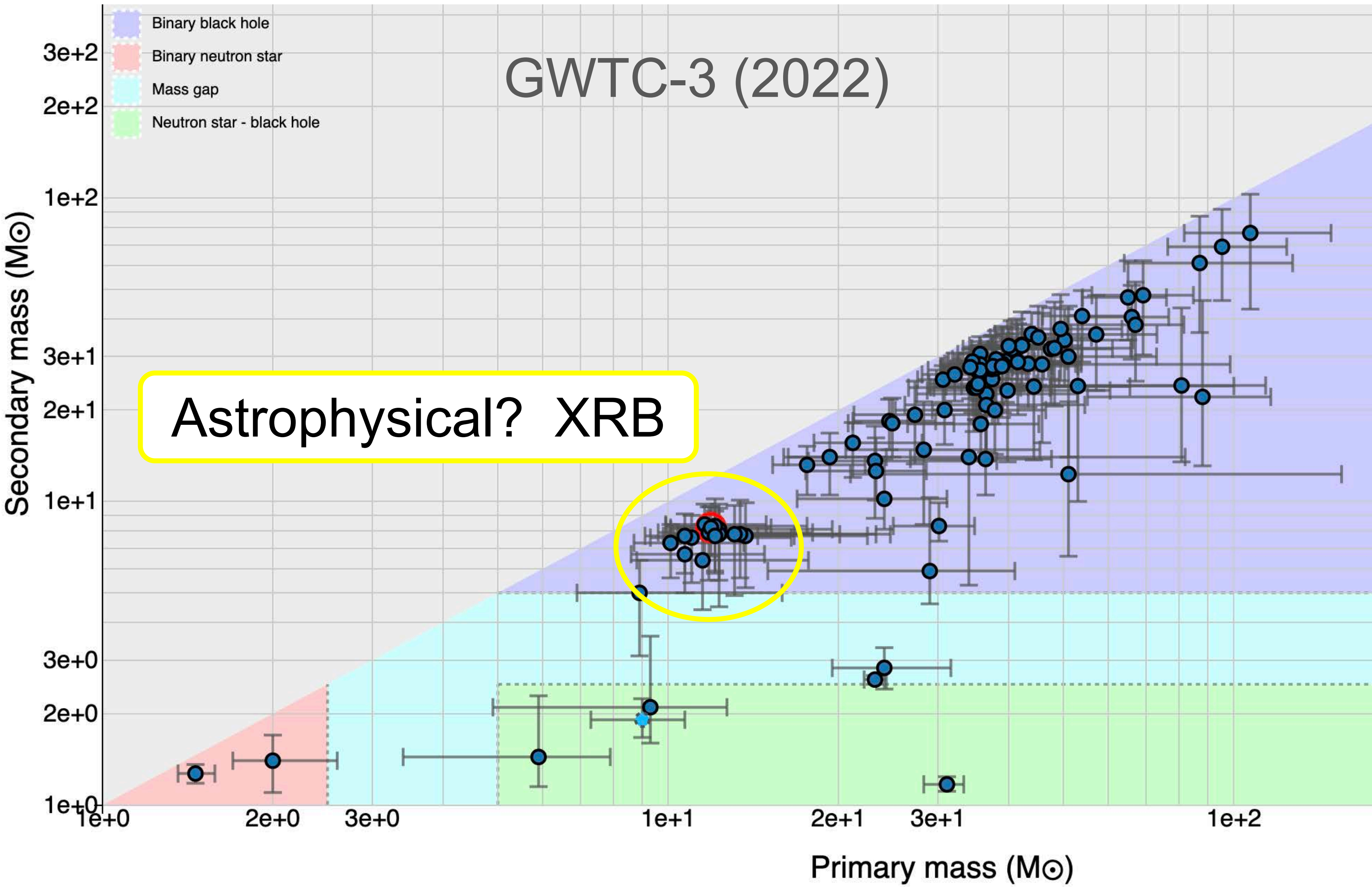

PBH clusters' merger rates

Trashorras, JGB, Nesseris [2006.15018]

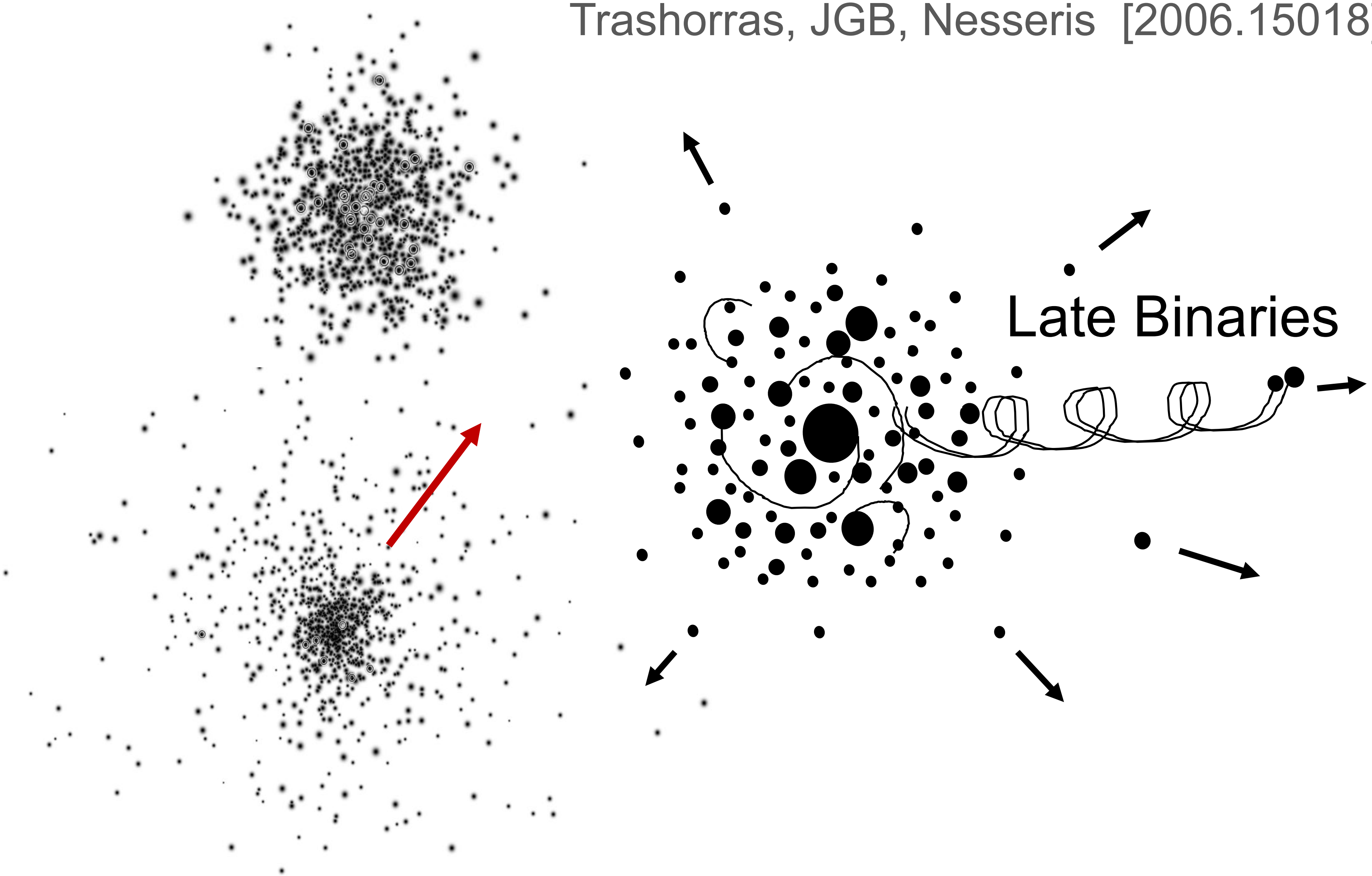

Are LIGO/Virgo BH Primordial?

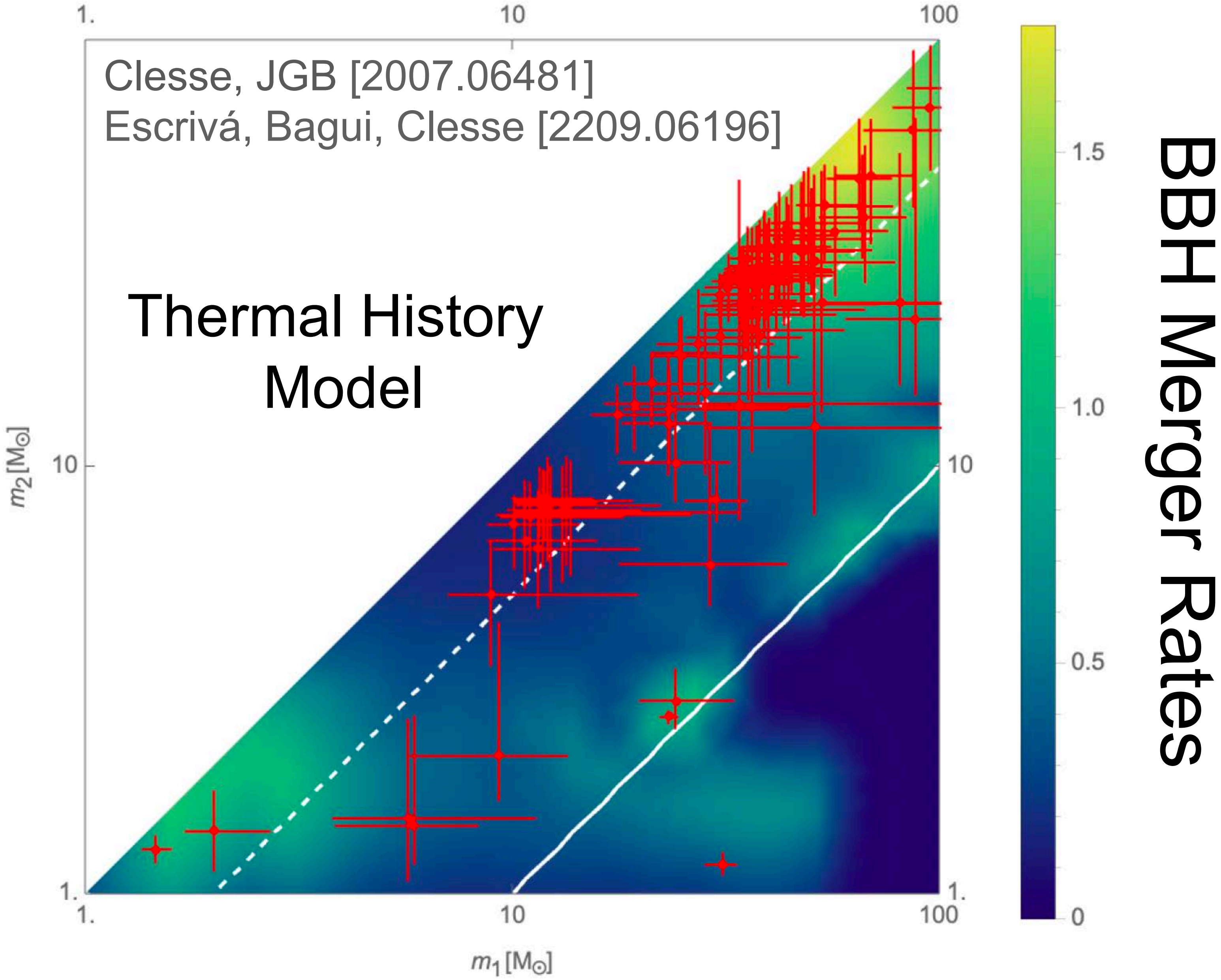

Effective and Final Spin

JGB – Phil.Trans.Roy.Soc.A 0091 (2019)

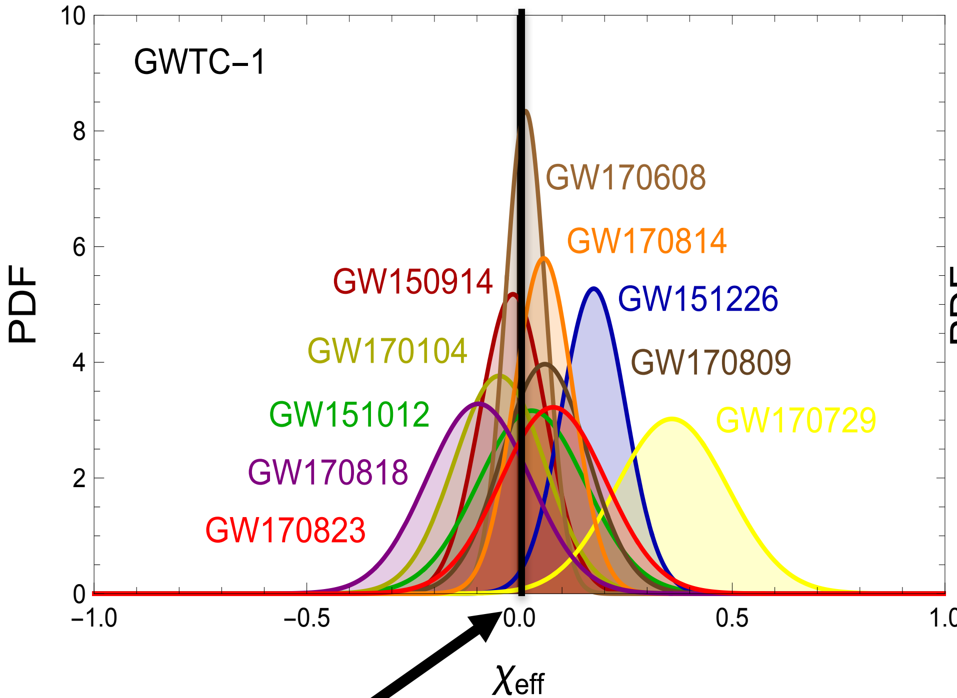

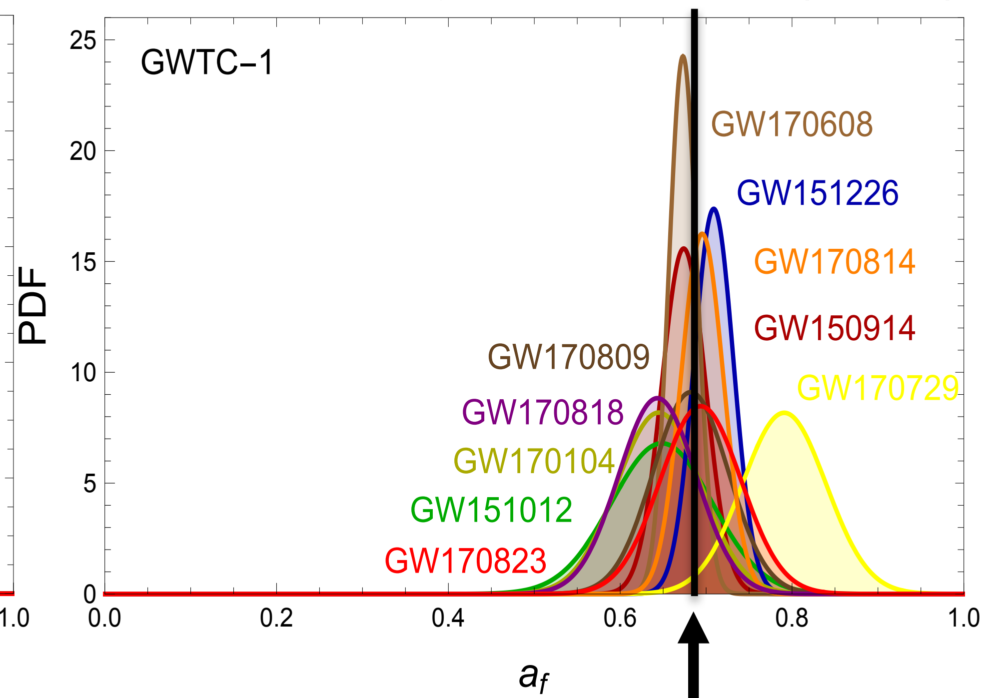

$$\chi_{\rm eff}(S_1 = S_2 = 0) = 0$$

$$a_f(S_1 = S_2 = 0) = 0.686$$

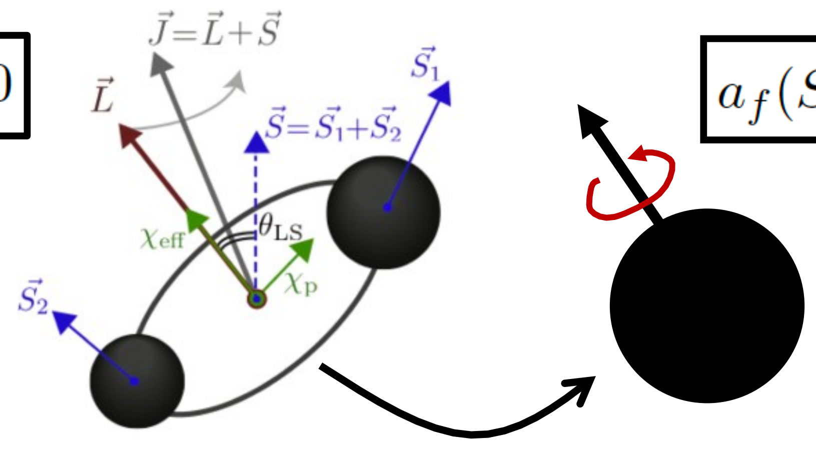

Effective and Final Spin

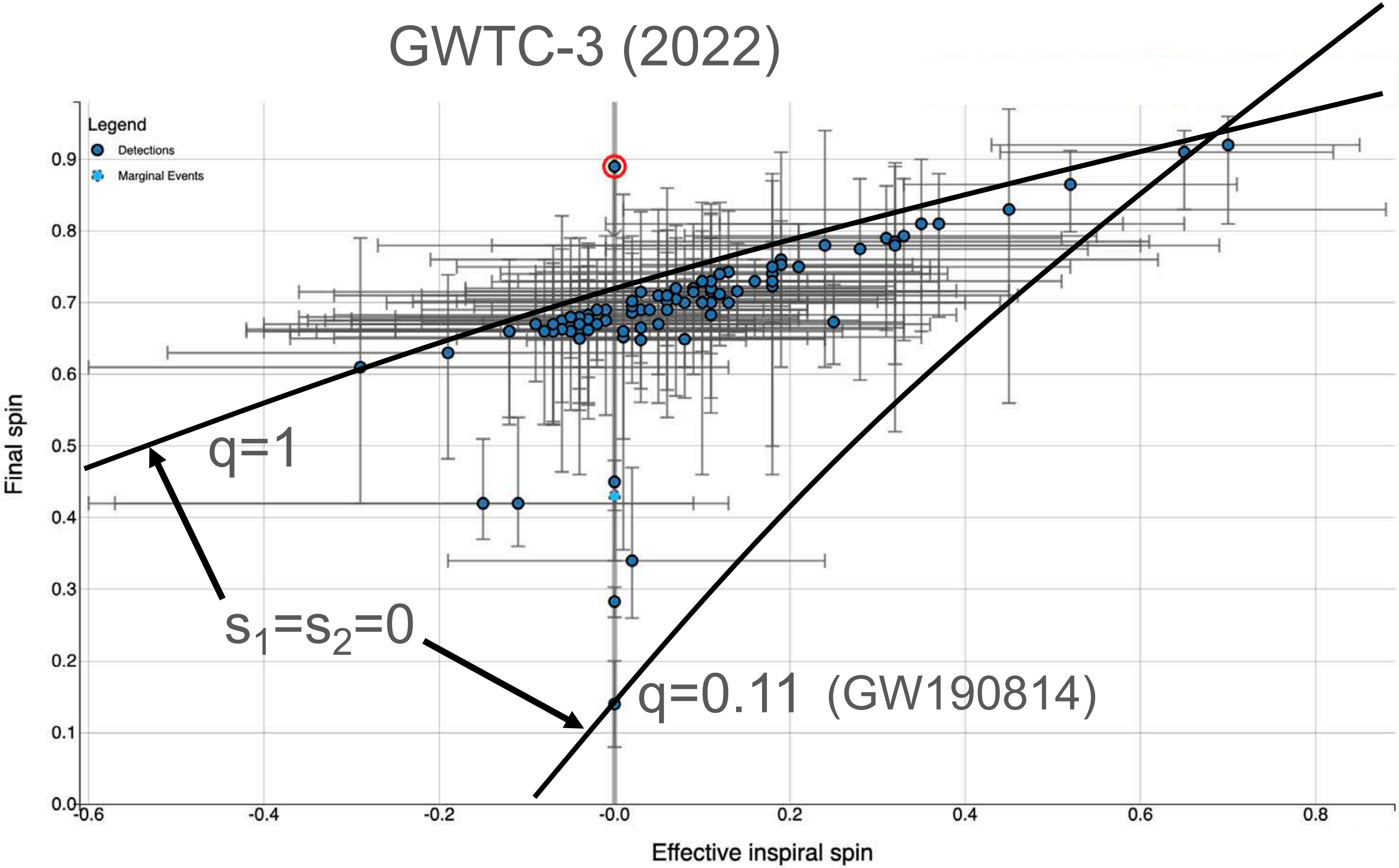

Effective and Final Spin

JGB, Nuño-Siles, Ruiz Morales [2010.13811]

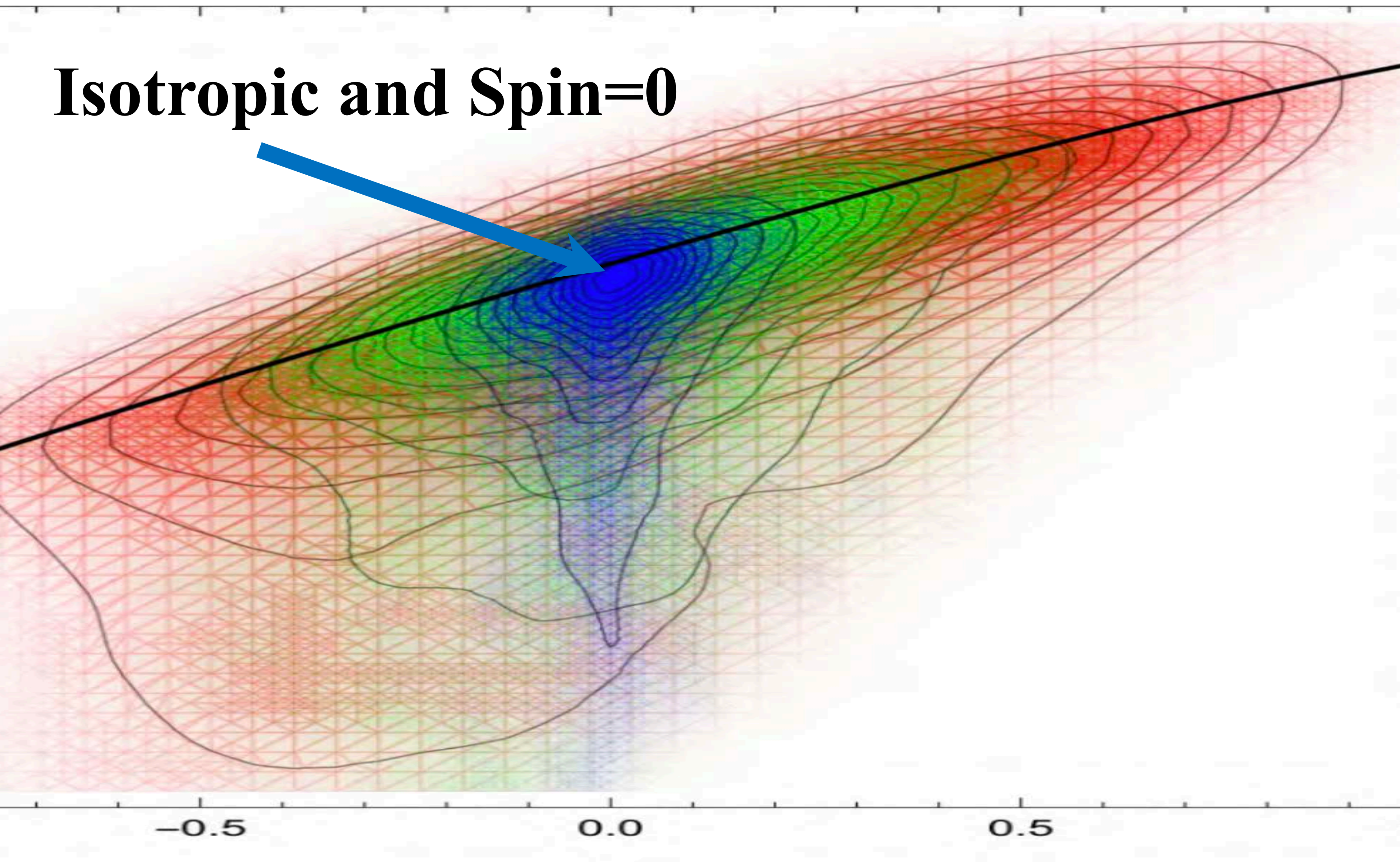

Spin induction in dense clusters

JGB, Nesseris [1706.02111]
“ [1711.09702]

Hyperbolic Encounters
(GW bursts)

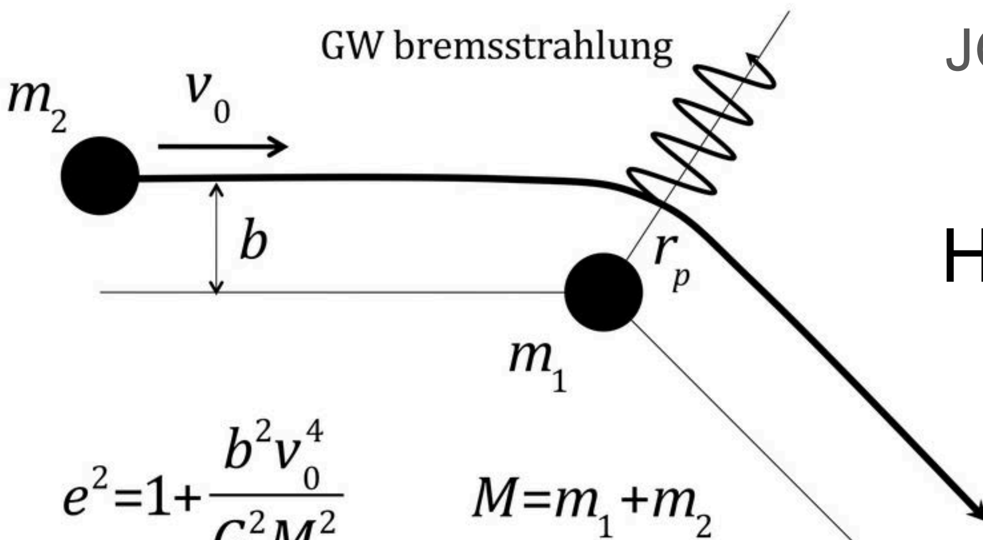

$$e^2 = 1 + \frac{b^2 v_0^4}{G^2 M^2} \qquad M = m_1 + m_2$$

Jaraba, JGB [2106.01436]

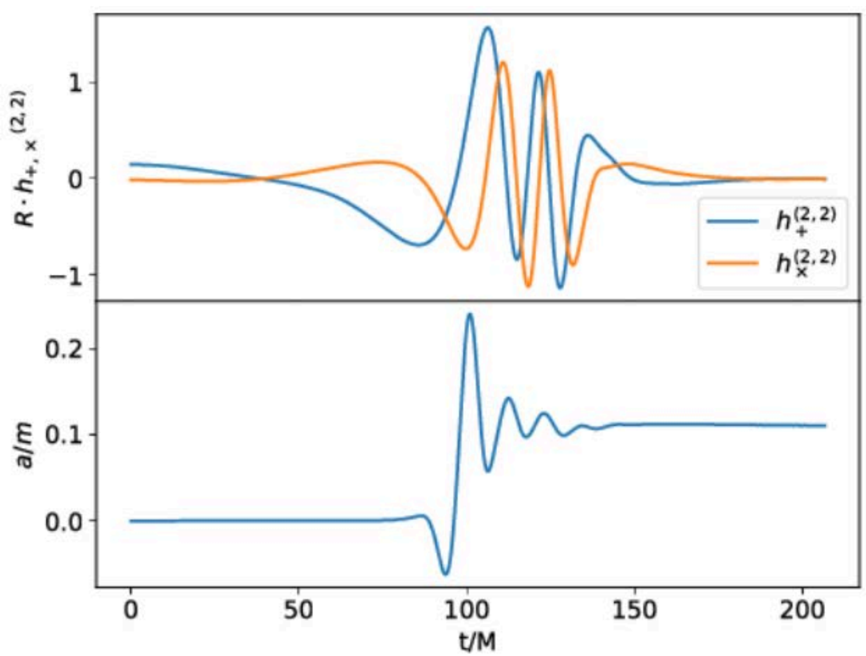

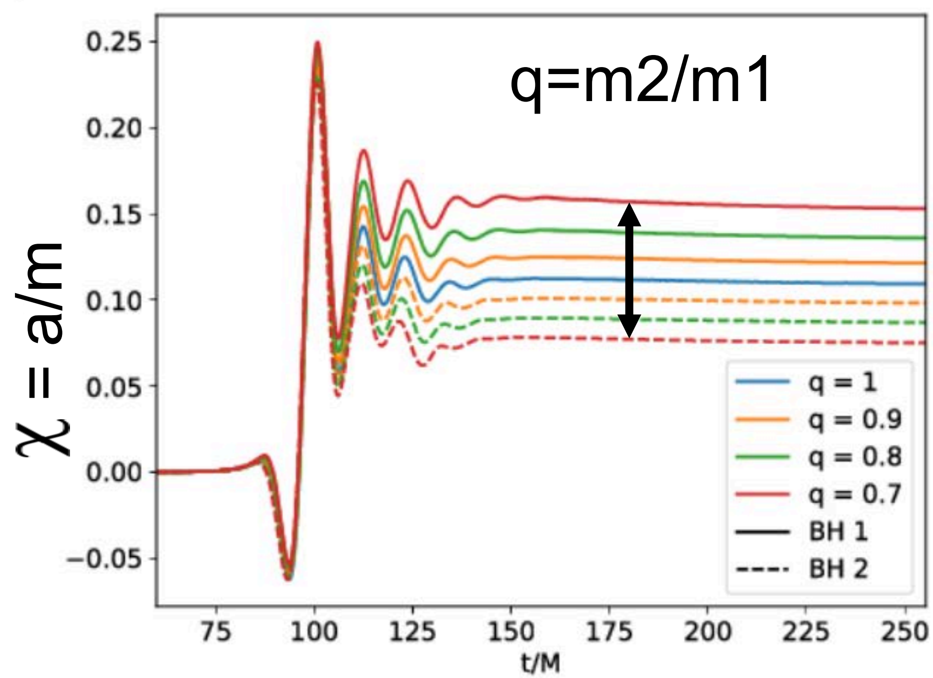

Spin distributions GWTC-3

LVK Collaboration [2111.03634]

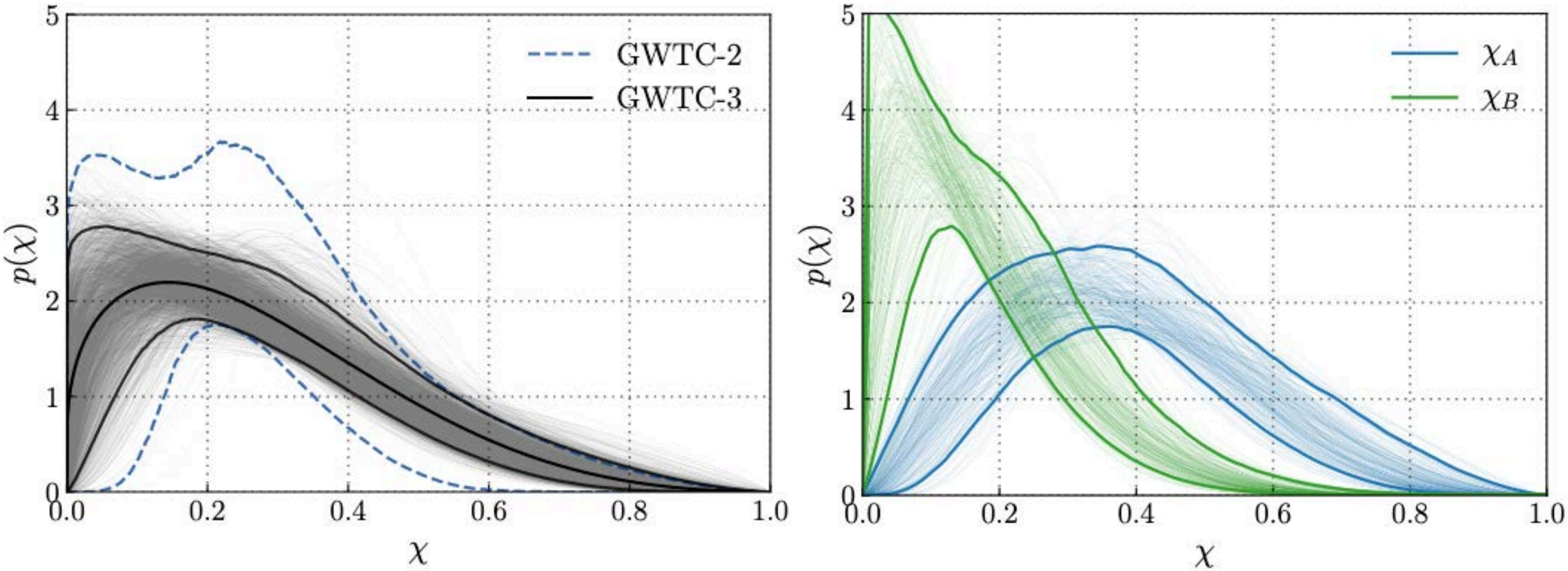

All component spins χ_1 and χ_2

$$\chi_A = \max_{|\chi|}(\chi_1, \chi_2)$$

$$\chi_B = \min_{|\chi|}(\chi_1, \chi_2)$$

Are LIGO/Virgo BH Primordial?

Morras et al. [2301.11619]

SSM170401

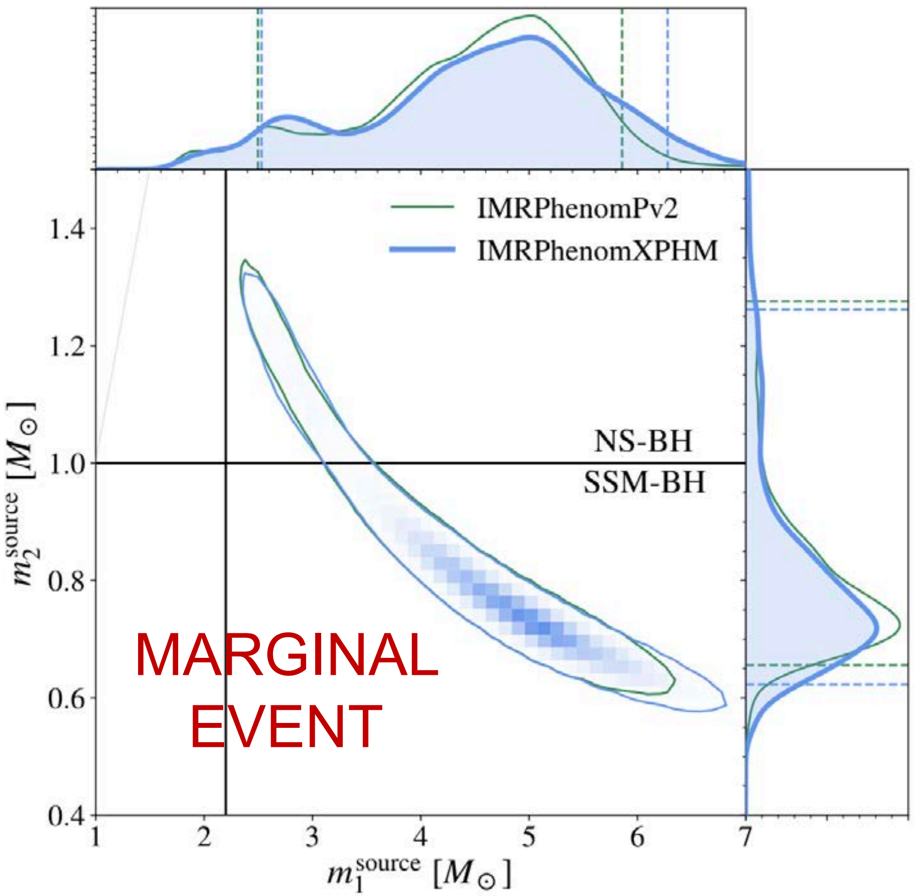

Parameter	IMRPhenomPv2	IMRPhenomXPHM
Signal to Noise Ratio	$7.98^{+0.62}_{-1.03}$	$7.94^{+0.70}_{-1.05}$
Primary mass ($M_\odot$)	$4.65^{+1.21}_{-2.15}$	$4.71^{+1.57}_{-2.18}$
Secondary mass ($M_\odot$)	$0.77^{+0.50}_{-0.12}$	$0.76^{+0.50}_{-0.14}$
Primary spin magnitude	$0.32^{+0.47}_{-0.26}$	$0.36^{+0.46}_{-0.30}$
Secondary spin magnitude	$0.48^{+0.46}_{-0.43}$	$0.47^{+0.46}_{-0.42}$
Total mass ($M_\odot$)	$5.42^{+1.10}_{-1.65}$	$5.47^{+1.43}_{-1.68}$
Mass ratio ($m_2/m_1 \leq 1$)	$0.17^{+0.34}_{-0.05}$	$0.16^{+0.34}_{-0.06}$
$\chi_{\rm eff}$ [51, 52]	$-0.06^{+0.17}_{-0.32}$	$-0.05^{+0.22}_{-0.35}$
$\chi_{\rm p}$ [53]	$0.28^{+0.34}_{-0.21}$	$0.33^{+0.33}_{-0.26}$
Luminosity Distance (Mpc)	119^{+82}_{-48}	124^{+82}_{-48}
Redshift	$0.028^{+0.018}_{-0.010}$	$0.028^{+0.017}_{-0.011}$
Ra (°)	-2^{+34}_{-35}	-1^{+34}_{-37}
Dec (°)	47^{+14}_{-26}	46^{+14}_{-29}
Final mass ($M_\odot$)	$5.34^{+1.11}_{-1.70}$	$5.40^{+1.45}_{-1.73}$
Final spin	$0.39^{+0.24}_{-0.07}$	$0.42^{+0.22}_{-0.10}$
$P(m_2 < 1\ M_\odot)$	85%	84%

Are LIGO/Virgo BH Primordial?

SSM200308

Prunier et al. [2311.16085]

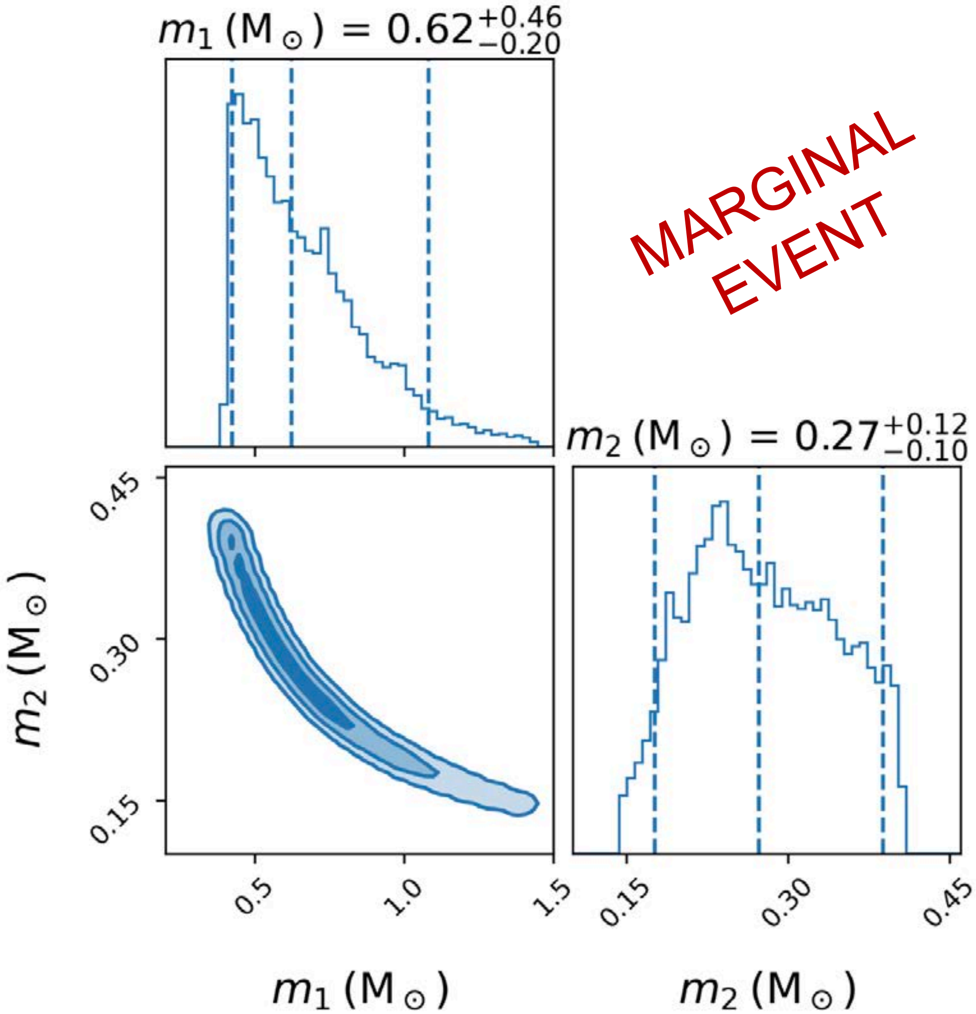

Parameter	
Matched Filter SNR	$8.02^{+0.49}_{-0.85}$
Primary mass ($M_\odot$)	$0.62^{+0.46}_{-0.20}$
Secondary mass ($M_\odot$)	$0.27^{+0.12}_{-0.10}$
Primary spin magnitude	$0.66^{+0.13}_{-0.25}$
Secondary spin magnitude	$0.44^{+0.33}_{-0.39}$
Total mass ($M_\odot$)	$0.88^{+0.35}_{-0.08}$
Detector-frame chirp mass ($M_\odot$)	$0.3527^{+0.0003}_{-0.0001}$
Mass ratio ($m_2/m_1 \leq 1$)	$0.44^{+0.48}_{-0.28}$
$\chi_{\rm eff}$ [27, 28]	$0.41^{+0.08}_{-0.04}$
$\chi_{\rm p}$ [29]	$0.37^{+0.24}_{-0.24}$
Luminosity Distance (Mpc)	90^{+43}_{-39}
Redshift	$0.02^{+0.01}_{-0.01}$
$P(m_1 < 1\ M_\odot)$	92%
$P(m_2 < 1\ M_\odot)$	100%

BBH sensitivity in future G3 GW

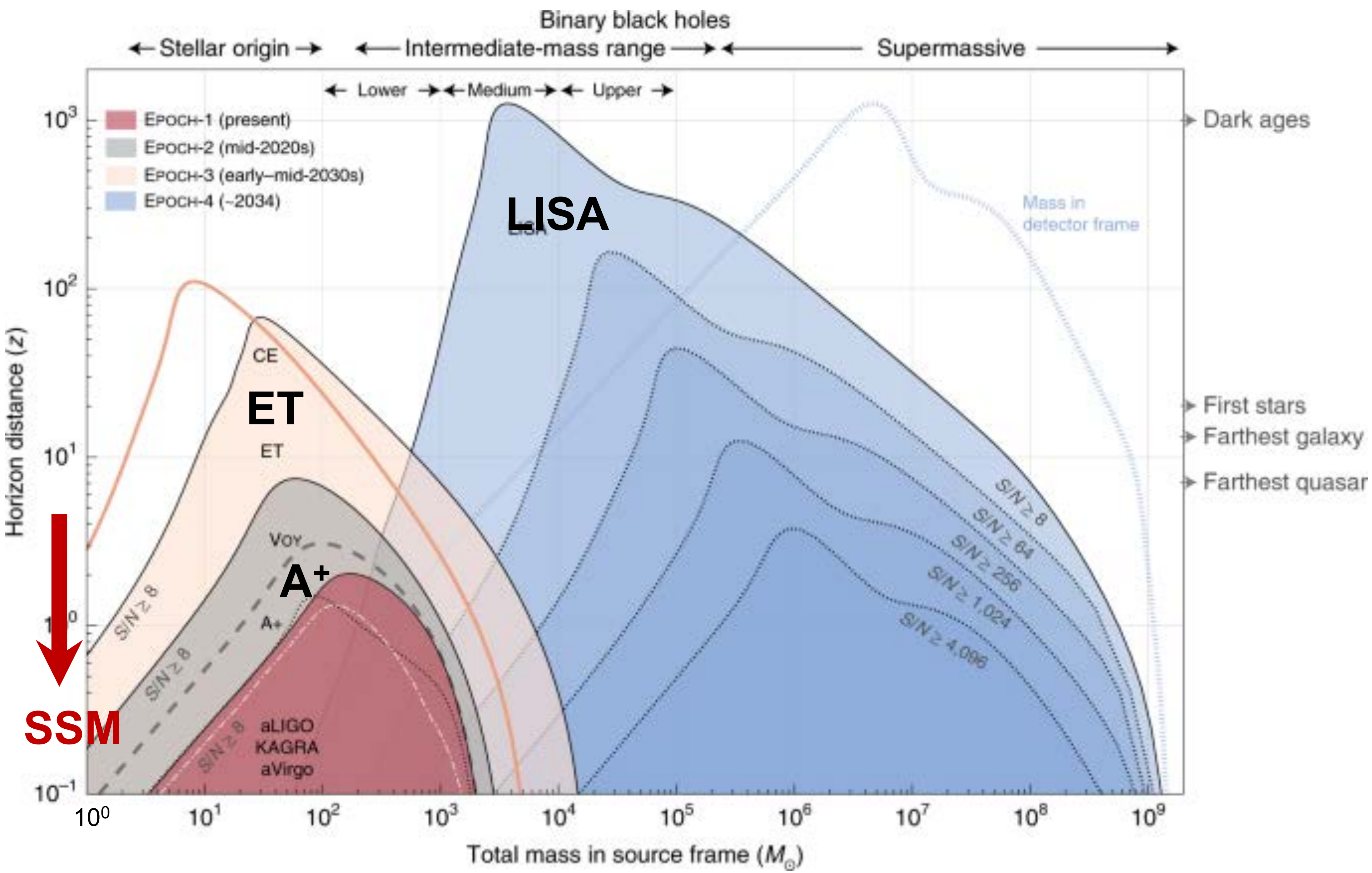

The future of GW (G3)

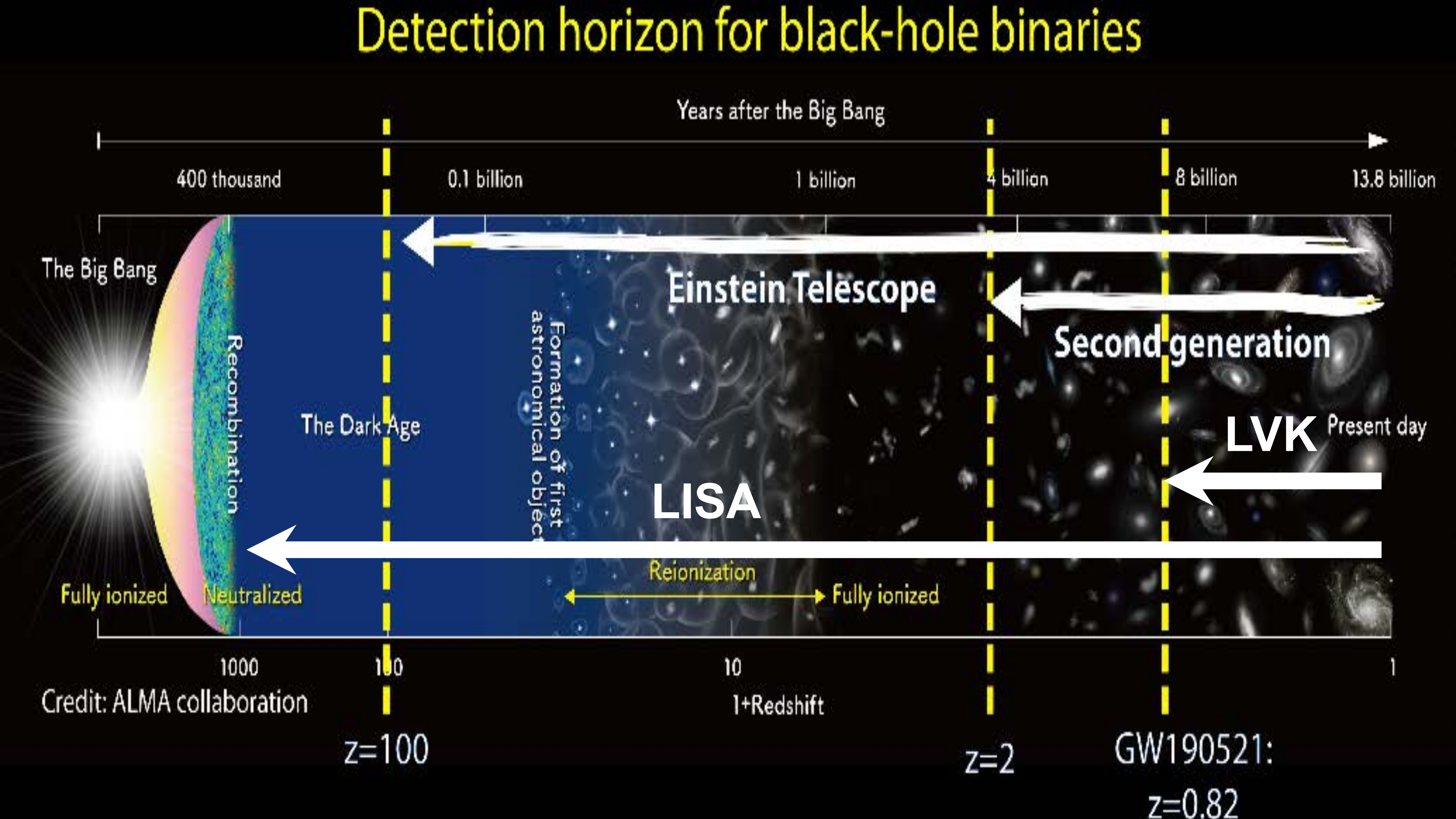

Conclusions

- Quantum diffusion inevitably generates PBH
- Thermal history predicts PBH with multimodal mass distribution $\sim 10^{-5}$, 1, 100, 10^{5} $M_{\odot}$ (10^{-10} $M_{\odot}$ also?)
- The predicted PBH spin and mass distribution has been measured by LIGO/Virgo + OGLE/Gaia around 1-100 $M_{\odot}$ (features: peak & plateau)
- Other peaks could be explored with LSST microlensing
- PBH scenario can explain various cosmic conundra
- Paradigm shift in Structure Formation of the Universe
- Very rich phenomenology: multiscale, multiepoch, multiprobe => Future G3 detectors (ET, CE, LISA)